

**Modeling of Distributed Generation under Next Generation
Interconnection Requirements**

Anna Edwards

A thesis

Submitted in partial fulfillment of the

requirements for the degree of:

Master of Science in Electrical Engineering

University of Washington

2016

Committee:

Daniel Kirschen

Richard Christie

Program authorized to offer degree:

Electrical Engineering

©Copyright 2016

Anna Edwards

University of Washington

Abstract

Modeling of Distributed Generation under Next Generation Interconnection Requirements

Anna Edwards

Chair of the Supervisory Committee:
Close Professor of Electrical Engineering, Dr. Daniel Kirschen
Electrical engineering

The amount of renewable energy and distributed generation is increasing in the distribution network and is changing the network from passive to active. IEEE is currently revising the interconnection Standard 1547 and in its project P1547 it is anticipated that the new version will include ride through requirements for distributed generation to enhance the stability of the system. Extending existing Wind and PV models with next generation controls evaluate the effectiveness of these new requirements. The extended PV model is added to an IEEE 34-node test feeder and the active distribution network's fault response is compared to the WECC simplified model for distributed PV system used for bulk system stability studies. It was found the draft IEEE P1547 ride-through requirements increase the amount of PV systems that remain connected post-fault. The parameters of the WECC simplified model for distributed PV systems are optimized to match the results from the IEEE 34-node test system with distributed PV. This allows the active distribution system to be simplified for bulk system stability studies and improves the computational performance.

Table of Contents

| | |
|---|-----|
| Abstract | iii |
| 1. Introduction..... | 1 |
| 1.1 Motivation | 1 |
| 1.2 Stability Impact of DER | 1 |
| 1.2.1 Technology | 1 |
| 1.2.2 Penetration and Location | 2 |
| 1.2.3 Interconnection Requirements | 3 |
| 1.3 Ride-Through Requirements | 4 |
| 1.4 Research Objective and Approach | 5 |
| 2. Extension of Existing Models..... | 7 |
| 2.1 Revision of the IEEE Std. 1547 | 7 |
| 2.2 Existing Dynamic DER Models | 9 |
| 2.3 Extension..... | 10 |
| 2.4 Wind model..... | 11 |
| 2.5 PV Model | 12 |
| 3. Implementation of WECC Simplified Model | 15 |
| 3.1 Simplified Models | 15 |
| 3.2 Testing | 17 |
| 4. Testing on a Typical North American Distribution Network | 22 |
| 4.1 North American Distribution Network | 22 |
| 4.2 IEEE 34-node Test System | 22 |
| 4.3 Results | 24 |
| 4.3.1 LVRT | 26 |
| 4.3.2 LVRT with Dynamic Voltage Support | 27 |
| 4.4 Optimize WECC Simplified Model | 29 |
| 4.5 Benefit of IEEE 1547 Standard | 33 |
| 5. Conclusion and Recommendations | 37 |
| Reference | 39 |
| Appendix A | 42 |
| Appendix B | 47 |

1. Introduction

1.1 Motivation

In August 2015, the President of the United States Barack Obama announced the Clean Power Plan. A step forward for the United States to address the problem of global warming, this plan calls for cutting carbon emissions 32% by the year 2030 [1]. One way to decrease carbon emissions is to add more renewable, non-carbon producing energy sources to the electricity system. Some of these new renewable energy sources are of a highly distributed nature and are connected to the distribution level. The insertion of these distributed energy resources (DERs) transforms the distribution network from a passive to an active part of the power system. Accurate modeling of the dynamic performance of these active distribution systems (ADS) are required to assess future power system reliability.

1.2 Stability Impact of DER

As DER penetration increases, it may have an effect on the dynamic behavior of the power system. This thesis considered the following factors: technology of the Distributed Generation (DG), penetration and location, and grid connection interface.

1.2.1 Technology

The type of technology of the DER affects its impact on stability. The impact on the duration of the rotor speed oscillations due to tripping of DERs depends on whether the power electronic converters are equipped with voltage and frequency control. DER with asynchronous generators has a lesser impact on transient stability. This is believed to be due to the opposite effects of near and remote generators counterbalance. DER with synchronous generators decreases the over speeding of large-scale generators. However, it also decreases transient stability by increasing the oscillation duration that may be caused by the inter-area oscillation

phenomenon. DG with power electronics decreases over speeding of generators because the power electronics disconnect during a fault. The lack of voltage ride-through could potentially lead to loss of DER power in a large region of the power system and cause a post-fault real power imbalance [2].

1.2.2 Penetration and Location

Traditionally the voltage is controlled so that along a feeder the voltage stays within an acceptable range. The location of a large amount of DG on the feeder can have a negative effect on voltage at the end of the feeder. If the DG is close to the beginning of the feeder it can confuse the line drop compensators and cause the voltage at the end of the feeder to be below the minimum voltage. If the DG is at the end of the feeder and the system is lightly loaded, it can cause the voltage at the end of the feeder to be above the maximum voltage.

A large penetration of DERs can also have a negative effect on the voltage stability of the system. According to [2], when the penetration of DER is large, system transients can cause large voltage drops at some nodes causing the DERs in the system to disconnect. Large penetration of DERs can also have an effect on the frequency stability of the system. According to [3], an under frequency situation may trigger the under frequency protection of multiple DERs. This is a common-mode failure, which is a failure of multiple devices in a power system stemming from a single event. This may lead to massive tripping of more DERs that may lead to an even larger frequency drop. An over-frequency situation may trigger DERs over frequency protection and could cascade into an under frequency situation. The lack of frequency ride-through of DER increases the risk of under-frequency load shedding. This research, only studies the effects of voltage stability on the system.

1.2.3 Interconnection Requirements

Interconnection requirements determine the performance of DERs under certain conditions. IEEE Std. 1547-2003 is the de-facto interconnection standard in the U.S. In its current version, it does not require voltage or frequency ride-through. On the contrary, it actually requires a mandatory trip of DERs for certain abnormal voltage or frequency conditions.

As summed up by an EPRI white paper [3] the lack of ride-through is an issue when a fault occurs on a system with a high level of DERs. Ride-through is defined as “the ability of a DER to remain connected to the grid after a disturbance without being tripped and being able to automatically restore its current output quickly after a disturbance.” Several standards have been developed to specify ride-through and relay-setting requirements. These standards include NERC Standard PRC-024-02, WECC VRT, FERC order 661-A, and IEEE Std. 1547-2003. This thesis, examines next generation Low Voltage Ride-Through requirements for DER to see how they affect the stability of the system and to investigate to what extent they can be modelled in bulk system stability studies.

Table 1 gives the system response requirements due to abnormal voltages. The DER will stop energizing the area within the clearing times indicated.

Table 1: IEEE Std. 1547-2003 voltage trip requirements [4].

| Voltage range (% of base voltage) | Clearing Time (s) |
|--|--------------------------|
| V<50 | 0.16 |
| 50≤V<88 | 2.00 |
| 110<V<120 | 1.00 |
| V≥120 | 0.16 |

Table 2 gives the clearing time values for a frequency outside the normal range. The clearing times are also dependent on the size of the DER.

Table 2: IEEE Std. 1547-2003 frequency trip requirements [4].

| DR size | Frequency range (Hz) | Clearing Time (s) |
|----------------------|--|--------------------------|
| $\leq 30 \text{ kW}$ | >60.5 | 0.16 |
| | <59.3 | 0.16 |
| $>30 \text{ kW}$ | >60.5 | 0.16 |
| | <\{59.8-57.0\} (Adjustable set point) | Adjustable 0.16 to 300 |
| | <57.0 | 0.16 |

1.3 Ride-Through Requirements

According to the same EPRI white paper, the considerations for voltage tolerance requirements include the following [3]:

- The location of each DER needs to be taken into account and how it affects the voltage drop.
- How much the voltage will drop based on the amount of DERs in the system.
- How long it will take a fault on the system to clear.
- How long it will take the voltage to return to normal.
- These requirements should allow for fast post-fault power recovery. Requiring high-voltage ride-through (HVRT) should prevent further tripping [3].

The objective of a minimum frequency ride-through requirement is to avoid excessive loss of generation from DER following a frequency disturbance. According to the EPRI white paper, the requirements for frequency tolerance requirements include the following [3]:

- Tripping should not occur before under-frequency load shedding.
- Tripping should not occur during an over-frequency event.
- Tripping should follow minimum ride-through requirements based on internal protection functions.
- Frequency ride-through requirements should maintain a minimum rate of change [3].

When looking at fault ride-through requirements some additional considerations to take into account include the risks of allowing exceptions to the rules. There should not be exceptions created for some DERs, an exception could worsen the stability of the power system [5]. In addition, in order to maintain the real power balance and frequency stability after a disturbance, there should be a fast restoration to the pre-fault real power output levels [6]. Other considerations taken into account when dealing with DERs are manufacturing challenges in offering products in a competitive global market. When implementing ride-through requirements it should not have an impact on the owners of the DER and the requirements should not lead to increased cost for the owners. Finally, the effect on electric powers systems operators varies depending on if they are operating the system in LVRT or LVRT with dynamic voltage support [3] explained in section 3.2.

1.4 Research Objective and Approach

The objective of this study was to develop dynamic equivalents for North American active distribution systems with large amounts of DERs that comply with next generation interconnection standards for use in bulk system stability studies. The first step was to extend the existing models to model the next generation ride through standards. The second step was to implement and verify a simplified model developed by the Western Electric Coordinating Council (WECC). The third step was to set up a typical North American Distribution network with high amounts of DERs. The fourth step was to optimize the WECC Simplified model results to match the more elaborate North American distribution network results.

This thesis used DIgSILENT PowerFactory™ to perform the stability modeling of the power system. PowerFactory has unique capabilities to perform stability type (rms) simulations for power system with distributed energy resources, both with positive-sequence and phase

representation of the network and for a number of scenarios and study cases [7]. Other programs considered were Power-WorldTM, Grid Lab-D, PSS/eTM, and PSLFTM.

2. Extension of Existing Models

2.1 Revision of the IEEE Std. 1547

IEEE Standard 1547 is currently under full revision by the IEEE Standards Association's Working Group P1547. EPRI is facilitating the drafting of ride-through requirements in collaboration with the power industry. The aforementioned EPRI White Paper [3] contributed to these discussions. One of the key recommendations is to differentiate the ride-through control modes depending on operating regions based on the applicable voltage as illustrated in Figure 1.

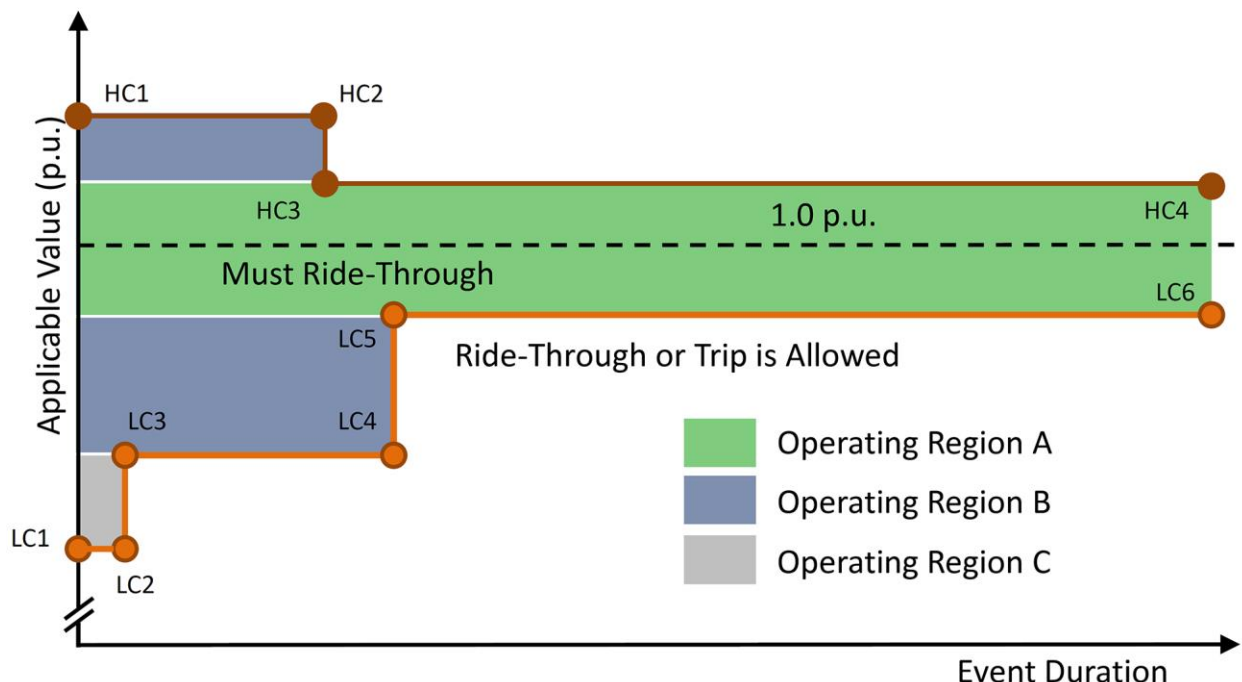


Figure 1: Differentiation of Ride-Through Modes Depending on operating regions based on the applicable voltage [3].

The latest working document of IEEE P1547 (draft 3) [8] considers the idea of multiple control modes during ride-through. The four control modes to differentiate are:

1. “Continuous Operation” remain in normal operating mode.
2. “Mandatory Operation,” this means either continuing with the pre-fault operation mode when in steady state or providing dynamic reactive support by adding additional reactive current injection.

3. “Momentary Cessation,” which stops any current exchange in the network.
4. “Permissive Operation,” which can be either mode two or three.

The motivation behind adding a “Momentary Cessation” requirement is that if the voltage has a large dip it probably means that the fault is close to the DER and in which case it should not inject current into the system as to avoid coordination issues with local protection schemes.

The IEEE P1547 parameters used for the PV and wind model extension are illustrated in Figure 2. This is the proposed IEEE P1547 standard category III based on the CA rule 21 and Hawaii explained in [9] and [10]. The models will use the category III standard values for all the simulations in this thesis [3]. Along the vertical axis is the voltage per unit and along the horizontal axis is the time in seconds on a logarithmic scale. Then depending on the voltage drop and the time of the fault will dictate how the model responds.

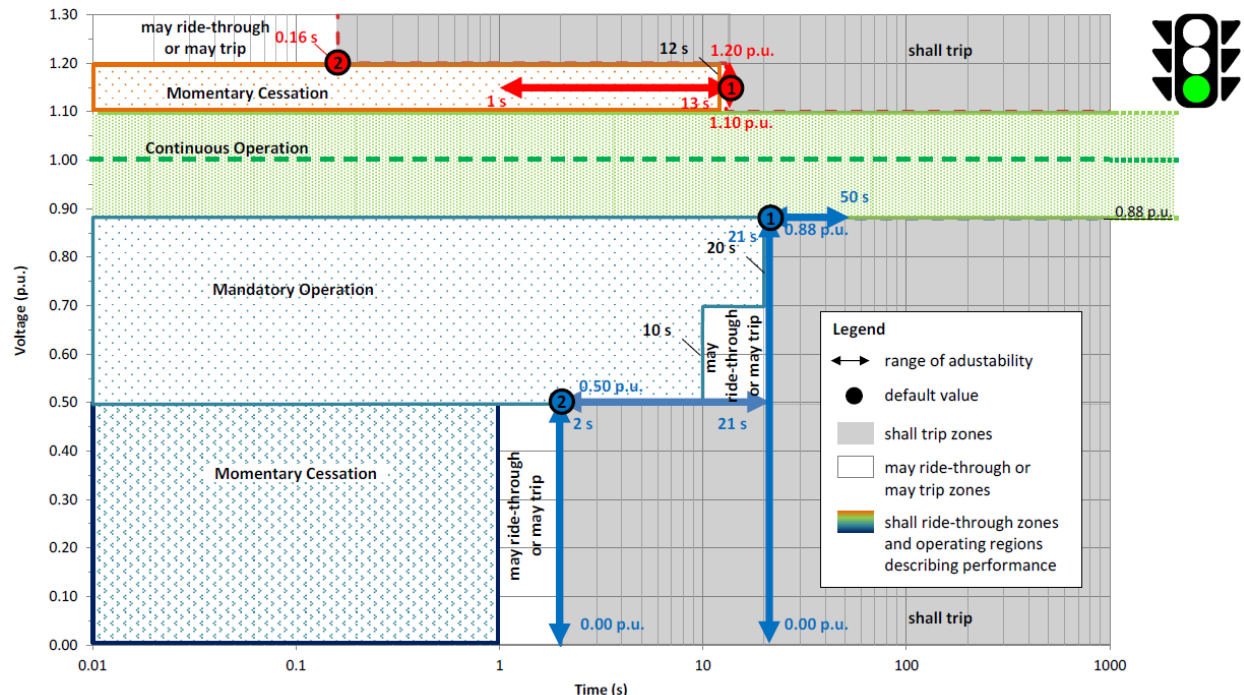


Figure 2: Proposed updates for IEEE P1547 [3].

2.2 Existing Dynamic DER Models

The challenging aspect of modeling of a wind turbine is that the specific models developed by the manufacturers are not in the public domain. Therefore, generic models are often used with standard parameters given in DIgSILENT PowerFactory. Figure 3 shows the generic International Electrotechnical Commission (IEC) model as specified in the International Standard IEC 61400-27-1 [11]. The IEC developed the wind power generation model to provide a generic dynamic model that can be used in power system stability studies. This model is used to study large-disturbance short-term voltage stability phenomena and to study other short-term dynamic phenomena such as rotor angle stability, frequency stability and small-disturbance voltage stability [11].

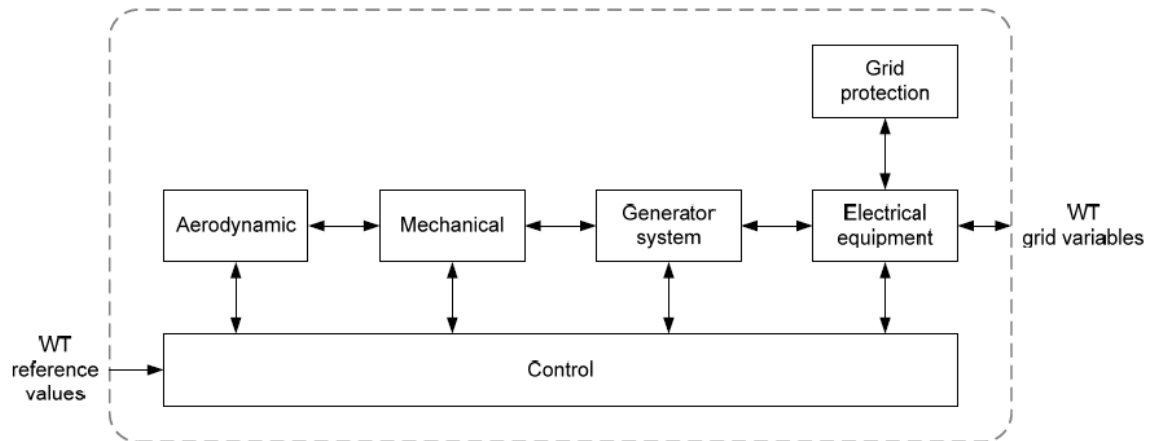


Figure 3: IEC Wind model [11].

The IEC model has the following limitations [11]:

- It does not support long-term stability analysis, the investigation of sub-synchronous interaction phenomena, or dealing with turbulence, tower shadow, wind shear and wakes.
- It does not cover phenomena such as harmonics.
- It does not include controls and additional equipment.
- It does not include short circuit calculations and studies with extremely weak systems.

Nanou and Papathanassiou proposed a grid-code compatible PV system model with LVRT capability suitable for power system dynamic and transient analysis studies [15]. The key aspects of this model is that it includes control features that provide immunity to voltage dips and regulation of output current to meet requirements for grid voltage support.

DIgSILENT has already implemented four different types of IEC models [12]. These models can be loaded and used to run simulations. The IEC models are encrypted “black box” models in DIgSILENT PowerFactory, so this project uses the “white box” models based on [13] and [14].

2.3 Extension

Since the current models do not use the concept of voltage-dependent operating regions, i.e., they either ride through or drop out during a disturbance, there is currently no way for the system to go from mandatory operation to momentary cessation. The goal of extending the existing dynamic models is to understand how the models work and to incorporate the proposed IEEE P1547 standard updates.

When extending the existing models, the first thing done was to add a second deadband, named FRT_db_LOW and deadband_low for the wind and PV models respectively. The low deadband determines when the model goes from mandatory operation to momentary cessation. It does this by having the model switch from LVRT with dynamic voltage support in the mandatory operation mode to LVRT in the momentary cessation mode when the voltage drops below the low deadband. This allows the system to remain connected and to recover post-fault as long as the voltage recovers within the time limit. For all the simulations run in this study, the lower deadband was set to 0.5pu because in Figure 2 this is the values on the vertical axis when the model is supposed to switch from mandatory operation to momentary cessation.

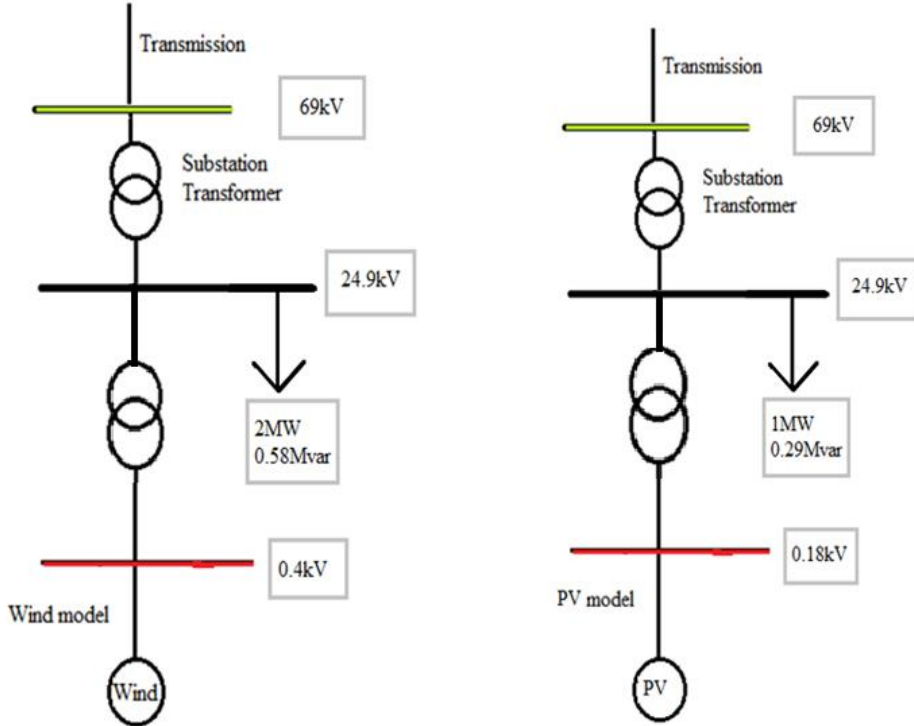


Figure 4: Wind and PV test systems.

2.4 Wind model

The test system used to verify extended wind generation model is on the left side of Figure 4. The wind turbine produces 2MW of power at a voltage level of 0.4kV. The wind turbine transformer then steps the 0.4kV voltage up to the 24.9kV voltage of the distribution system. The parameters used for the wind model are the LVRT values in Table 6 in Appendix A. The load in the system is a complex load with 68% of induction machines consuming 2MW at a power factor of 0.96. The substation transformer uses the values found in the IEEE 34-node test feeder documentation [16].

Applying two different voltage drops validated the extension of the wind model. The first voltage drop was 0.35pu (retained voltage of 0.65pu) seen in the top three graphs of Figure 5. The dark red dashed line show the system behavior before extension, while the lighter red line show its behavior after extension, and the blue dotted blue line represents the lower deadband

value. When retained voltage stays above the lower deadband, the system behaves identically to the base case scenario. The model is behaving as expected because it stays in mandatory operation and does not go into momentary cessation.

The second voltage drop was 1.0pu in the bottom three graphs in Figure 5. Since the voltage drop is now greater than the lower deadband, the model goes into momentary cessation. The voltage drop is now greater in the extended model and there is no reactive power is injected during the fault. The model is behaving as expected because it is going into momentary cessation.

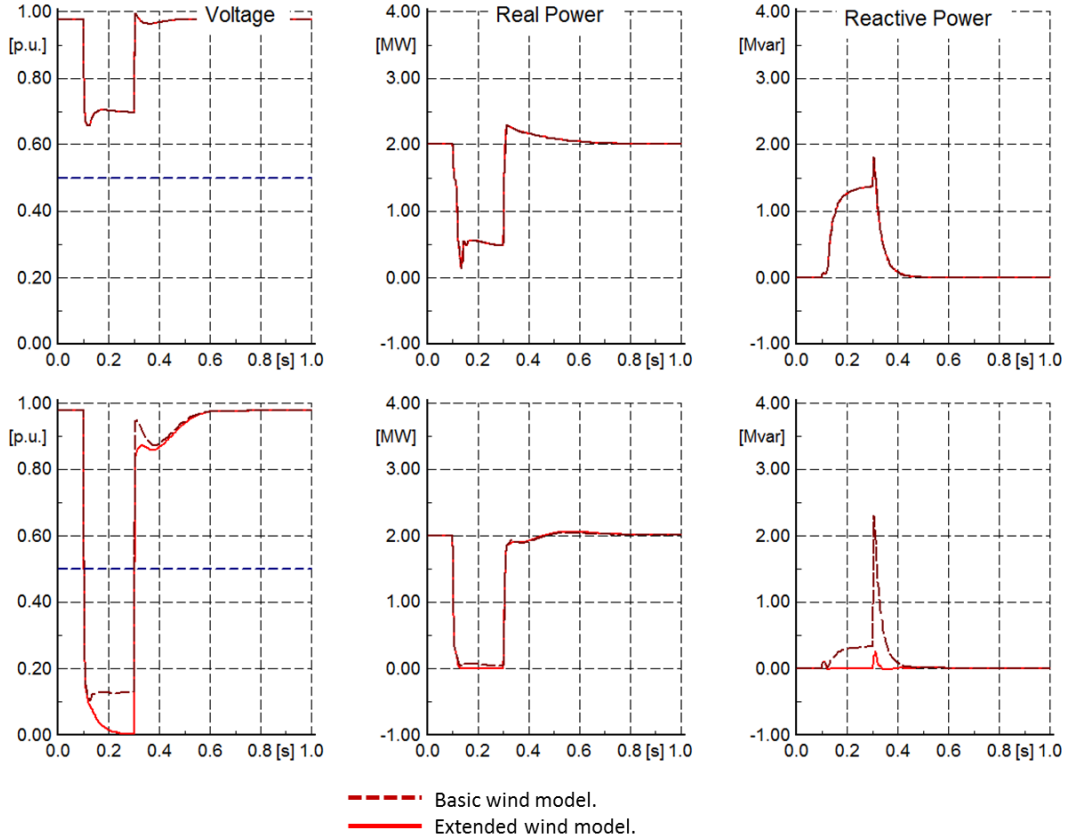


Figure 5: Results for wind model extension.

2.5PV Model

The test system used to verify the extended PV generation model is on the right side of Figure 4. The PV model represents 200 parallel solar panels. The reason for using 200 PV

panels is that a single PV panel of 10kW would have an insignificant impact and would not produce meaningful simulation results. Appendix B contains the procedure for increasing the number of PV panels in the model. The parameters used for the PV model are the LVRT with dynamic support values in Table 7 in Appendix A. The load in the system is a complex load with 68% induction machines consuming 1MW at a power factor of 0.96. The substation transformer uses the values from the IEEE 34-node test feeder documentation [16].

Applying two different voltage drops validated the extension of the PV model. The first voltage drop was 0.35pu (retained voltage of 0.65pu) seen in the top three graphs of Figure 6. The dark red dashed line is before extension, the lighter red line is after extension, and the blue dotted blue line represents the lower deadband value. The lower deadband is greater than the voltage drop so it behaves identically to the base case scenario. The model is behaving as expected because it should not go into momentary cessation.

The second voltage drop was 0.7pu (retained voltage of 0.3pu) in the bottom three graphs of Figure 6. Since the voltage drop is now greater than the lower deadband, the model goes into momentary cessation. The voltage drop is greater in the extended model and there no reactive power is injected during the fault. The model is behaving as expected because it goes into momentary cessation.

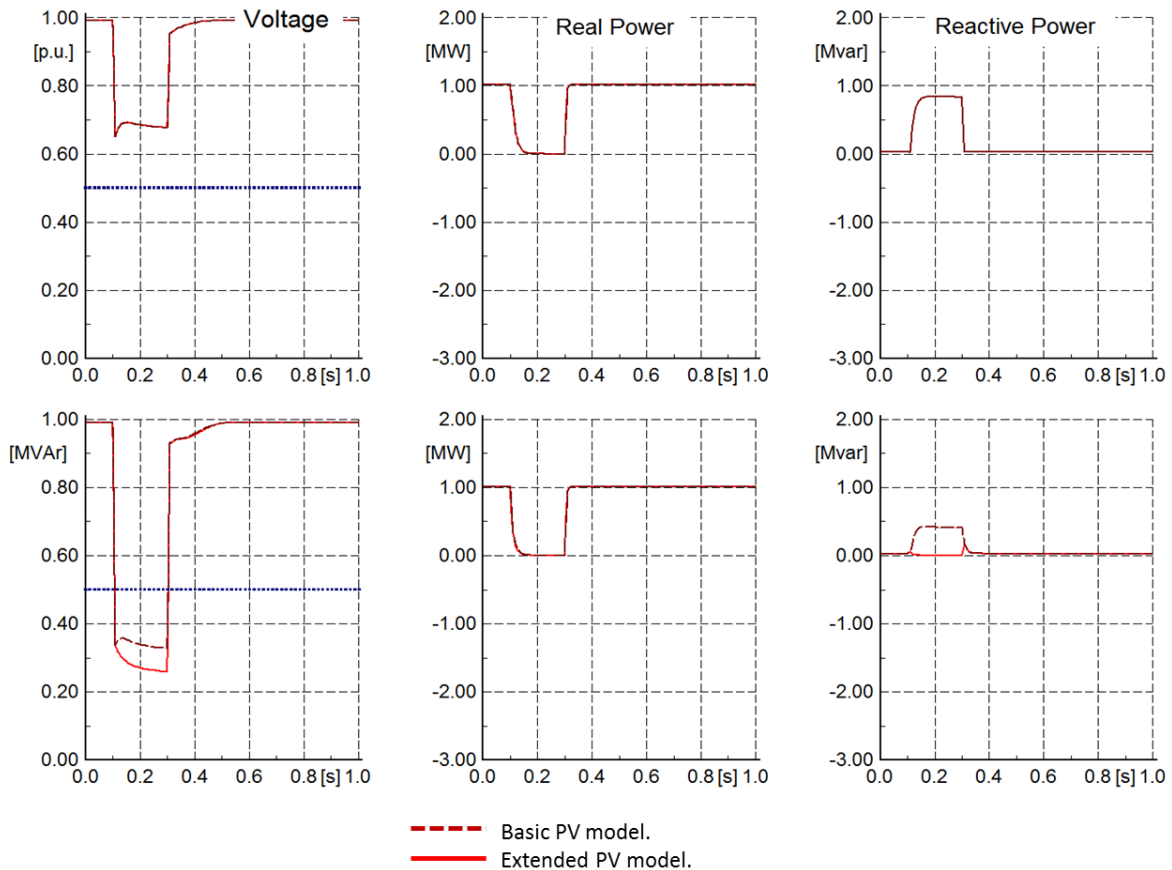


Figure 6: Results for PV model extension.

3. Implementation of WECC Simplified Model

3.1 Simplified Models

Some of the existing PV generation in The Western Electricity Coordinating Council (WECC) consists of small PV systems set up on a customer's premises and connected directly at distribution service voltage. The WECC distributed PV (PVD1) model is an aggregation of the PV models [17]. The aggregation decreases the high computational cost of modeling each individual PV generator. The model is a generator at the transmission network with an equivalent transformer and equivalent medium voltage feeder as shown in Figure 7. The large geographical area the PV panels may cover leads to each PV having a different electrical impedance between its terminals and the substation, leading to a diverse set of retained terminal voltages and therefore a different dynamic response of each individual PV system [17].

Recommended load flow model

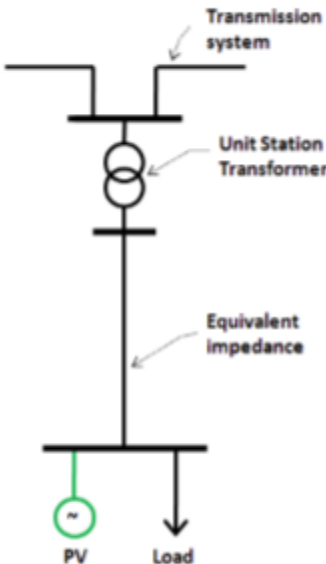


Figure 7: Test system for simplified WECC model [17].

Figure 8 shows the simplified WECC model block diagram. The default parameters provided are intended only for model testing and do not represent a particular implementation

[17]. For this thesis the most important block is the vrrecov. This block determines what percentage of the PV returns post-fault. When the voltage is between V_{t0} and V_{t1} a fraction of the power returns based on the voltage deviation.

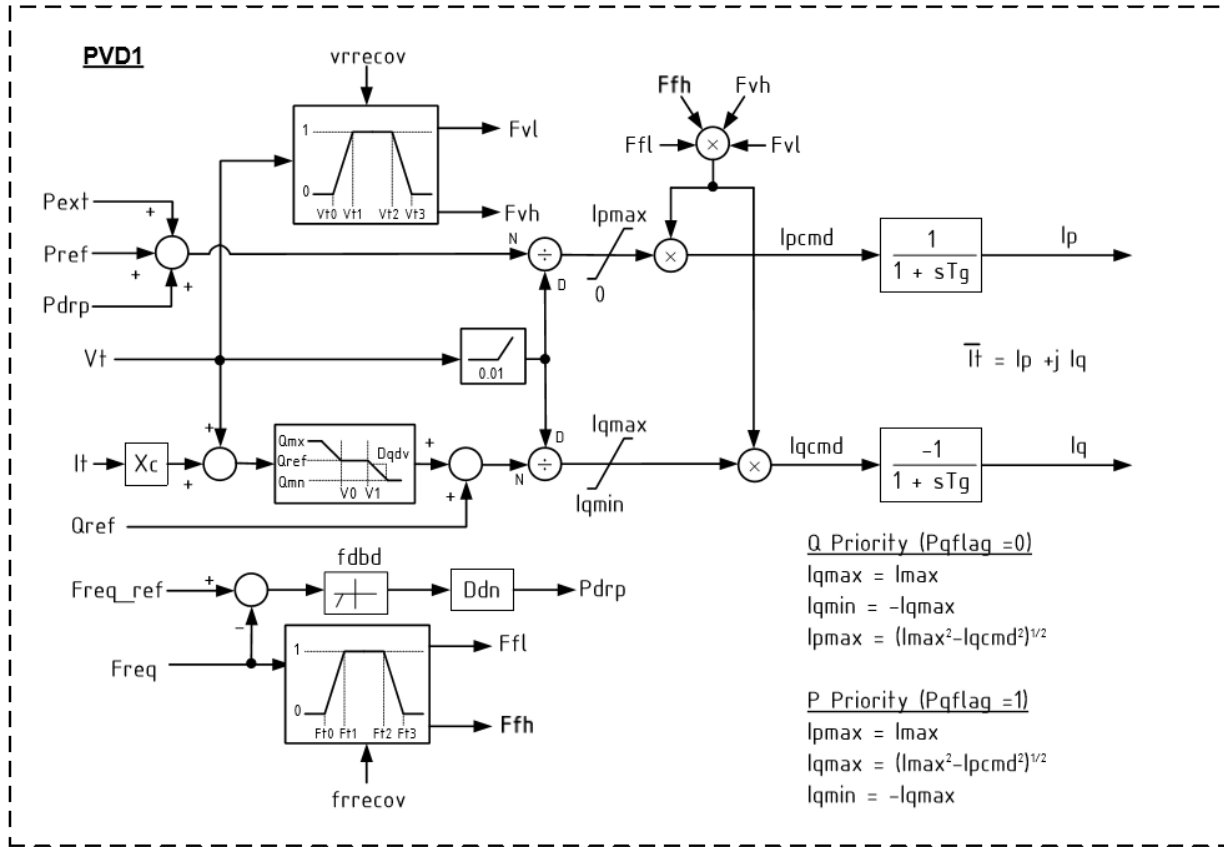


Figure 8: WECC simplified PV model [17].

The characteristics the simplified WECC model are [17]:

- It is not proprietary.
- It provides a good representation of the dynamic electrical performance of a PV.
- It is intended to study transmission grid faults.
- It focuses on the characteristics of dynamic recovery rather than system conditions during a fault.
- An equivalent representation and simplified dynamic models are not recommended for evaluation of fault ride-through.

- It assumes power flow is already solved.

The model allows for tripping of generation during a disturbance monitored at the aggregated PV terminal. The user can set the voltage and frequency deadbands to determine how much generation trips and what fraction of the generation returns post-fault. The PV model partial tripping setting is important because when PVs are aggregated each PV would experience the disturbance differently depending on its electrical distance from the fault [17]. The WECC simplified model limitations remain unexplored. A more sophisticated DER aggregation technique has been presented in [18].

3.2 Testing

The goal of implementing the WECC simplified model is to verify that the model is working and to compare its performance with the results obtained with a known model. Since the WECC model is an aggregated model, the best method of comparison is to compare it to the partial dropout of the extended PV models in a simple two-bus network.

Three different modes of the PV model were tested:

1. No Low Voltage Ride Through (nLVRT), which means when the retained voltage drops below 0.9pu the model assumes that the PV generation disconnects.
2. Low Voltage Ride Through mode (LVRT), which means that the PV generation will remain connected but will not provide dynamic voltage support.
3. LVRT with dynamic voltage support, which means that the PV will follow the proposed IEEE P1547 requirements presented in Figure 2.

Figure 9 shows the two-test systems used in this comparison the extended PV model setup is on the left and the WECC setup is on the right. The extended PV model with 50% partial dropout was setup by setting, at each bus, one PV model to nLVRT mode and one to

either LVRT or LVRT with dynamic voltage support. The parameters of the distribution line, load, and the substation transformer are from the IEEE 34-node test system [16]. The load consumes 2MW and 0.28Mvar to be consistent with the setting of the WECC simplified model. The PV model is set up to use constant voltage mode so that the steady state voltage deviation at the initialization would stay within the normal voltage band of be below 0.9pu to 1.1pu. Appendix B contains the procedure for switching the model to constant voltage mode.

The WECC simplified model was set up with 50% partial dropout, i.e., so that the model would have half the PV returning post-fault to match the extended PV model. The parameters for the WECC model setup also uses the parameters from the IEEE 34-node test system. The load is 68% induction motors and consumes 4MW at 0.98 power factor.

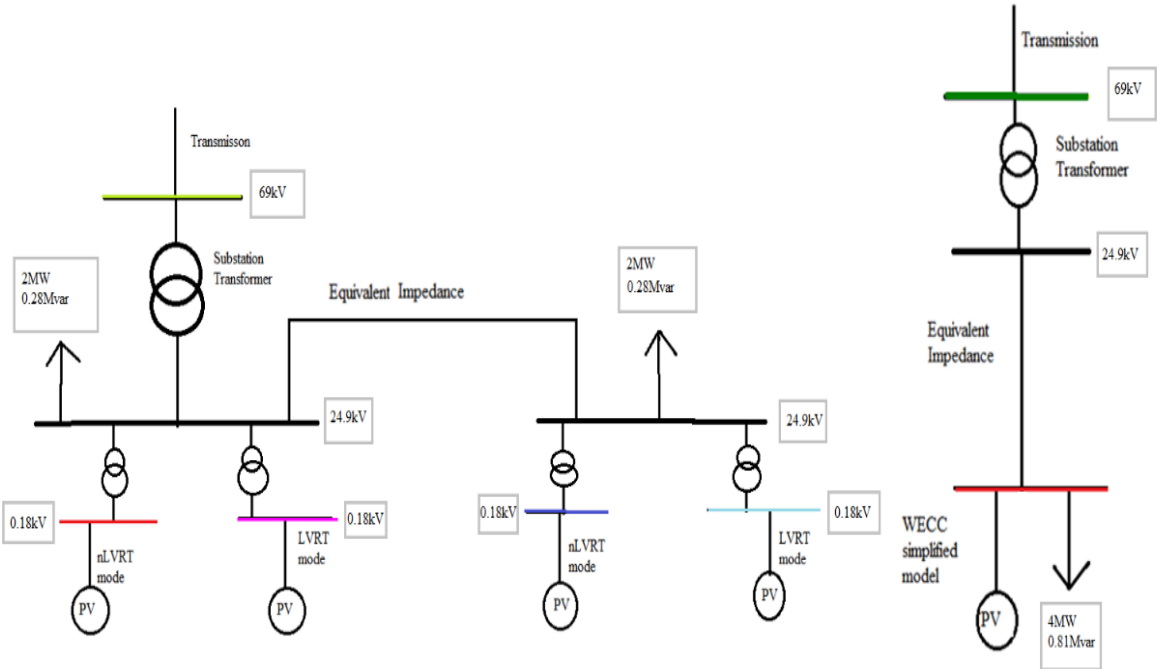


Figure 9: Partial dropout test systems.

Figure 10 shows the results for the simulation where the system is in LVRT without dynamic voltage support. The dark green line represents the value at the high voltage side of the

transformer for the WECC model while the light green line represents the values for the high voltage side of the transformer for the extended PV model with partial dropout model. The top three graphs show the results for a voltage drop of 0.35pu (retained voltage of 0.65pu) and the bottom three graphs show the results for a voltage drop of 0.7pu (retained voltage of 0.3pu). The real and reactive power pre- and post-fault match for both the models. While during the fault the real and reactive power does not match, it has the same shape. Changing the WECC simplified model line length would improve these results. Since the shape is the same and the pre- and post-fault power match, it can be assumed that the model was implemented correctly. Though one limitation of the WECC model is, it does not model what is going on during the fault. These parameters will be looked at in more detail in the testing chapter.

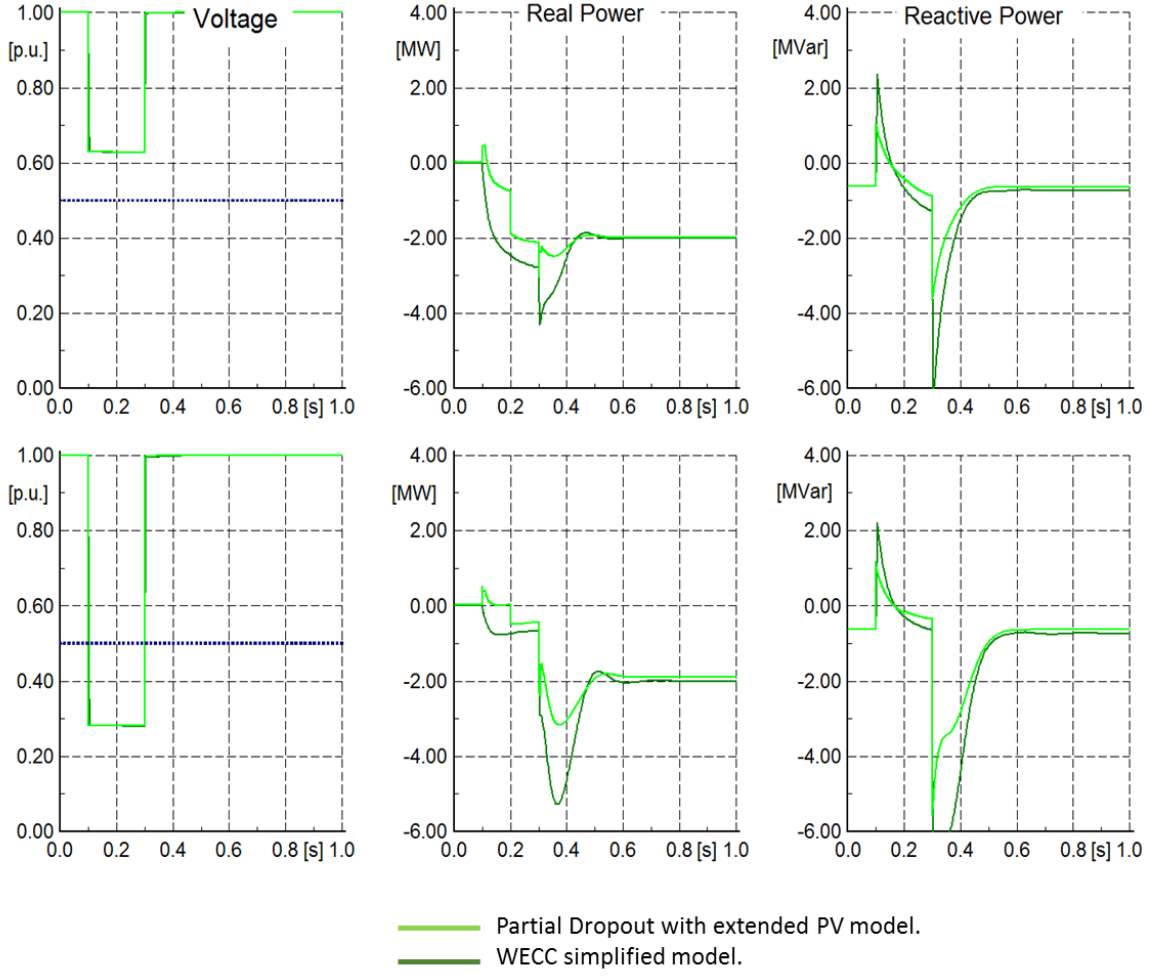


Figure 10: Results for LVRT partial dropout.

Figure 11 shows the results for the simulation run with LVRT with Dynamic Voltage Support. The difference from the LVRT mode is that it injects reactive power when the voltage drop to less than 0.5pu (retained voltage stays above 0.5pu). The dark green line represents the value on the high voltage side of the transformer for the WECC model while the light green line represents the values for the high voltage side of the transformer for the extended PV model with partial dropout model. The top three graphs show the results for a voltage drop of 0.35pu (retained voltage of 0.65pu) and the bottom three graphs show the results for a voltage drop of 0.7pu (retained voltage of 0.3pu). For the voltage drop of 0.7 pu the results look similar to the result for LVRT. While for the voltage drop of 0.35pu the post-fault real power values do not

match. The WECC model is an aggregated model, which explains the fact that it has more power returning for the smaller voltage dip (with higher retained voltage). The WECC model reduces the generation in amount proportional to the voltage deviation. . In this LVRT with dynamic voltage support case, the WECC parameters are 0.48pu and 0.90pu instead of 0.88pu and 0.90pu. Therefore, the partial dropout of the WECC model is much reduced compared to the pure LVRT case. Again, the WECC simplified model implementation seems to be correct based on these results.

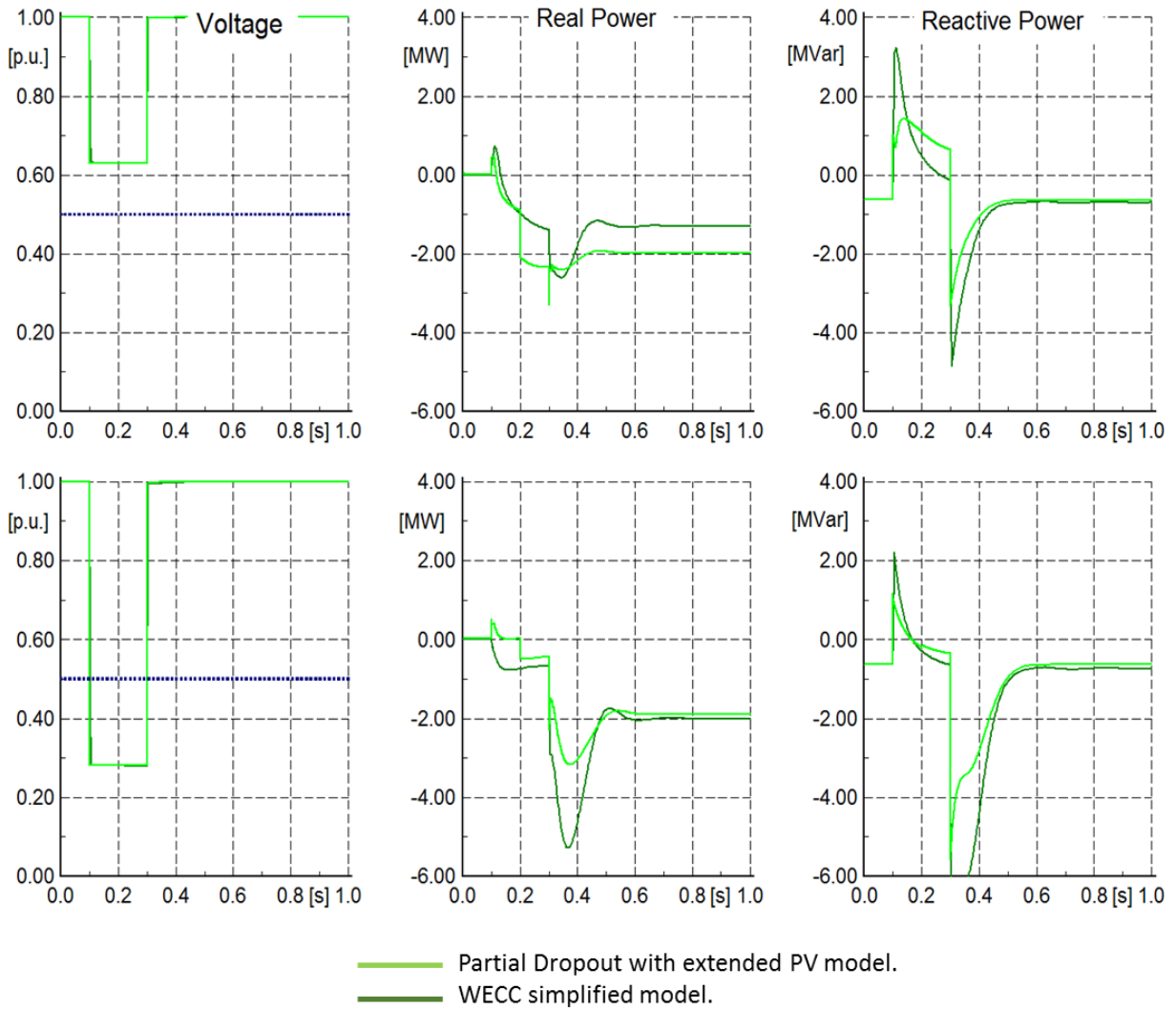


Figure 11: Results for LVRT with dynamic voltage support partial dropout.

4. Testing on a Typical North American Distribution Network

4.1 North American Distribution Network

The IEEE test feeders and a CIGRE benchmark system were considered to decide which system would be better for modeling of a typical North American distribution network in this thesis. CIGRE developed the CIGRE benchmark system to facilitate the analysis and validation of computational methods and techniques [19]. This thesis selected the IEEE 34-node test feeder shown in Figure 12. The IEEE 34-node test feeder was selected because the DigSilent PowerFactory student license has a 50-node limit and because it is based on an actual North American feeder, located in Arizona and with a nominal voltage of 24.9kV. Long and lightly loaded feeders, two in-line regulators, and an in-line transformer for a short 4.16kV section, unbalanced loading, and shunt capacitors characterized the IEEE 34-node test feeder. The total load for the feeder is 1.769MW and 1.044MVar [16].

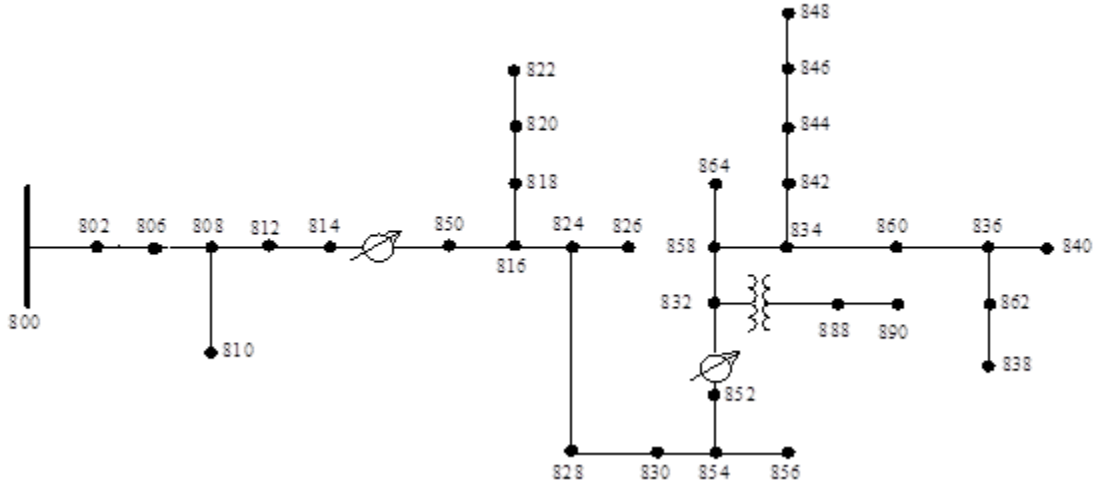


Figure 12: IEEE 34-node test feeder [16]

4.2 IEEE 34-node Test System

It was necessary to simplify the test system in order to stay under the 50 node DigSilent PowerFactory limit. To simplify the IEEE 34-node test system, one-half the distributed loads

were lumped at the end of the feeder. This model can be used to calculate the total voltage drop from the source to the end of the line with uniformly distributed loads. This model does not give the correct output for power loss calculation [20]. The new total power in the system is 1.408MW and 0.861MVar. This study looks at voltage drop so the simplification was determined acceptable.

To verify that the IEEE 34-node test feeder was set up correctly in PowerFactory the voltage at the buses are compared to the bus voltages given by IEEE [16]. Figure 13 is a heat-map for the voltage for each bus. The values in Appendix A in Table 9 show the percent error between the IEEE voltages and the voltages calculated by PowerFactory. The highest voltage difference is 4.16% and the average difference is 0.66%. This voltage difference was determined to be small enough to continue with testing.

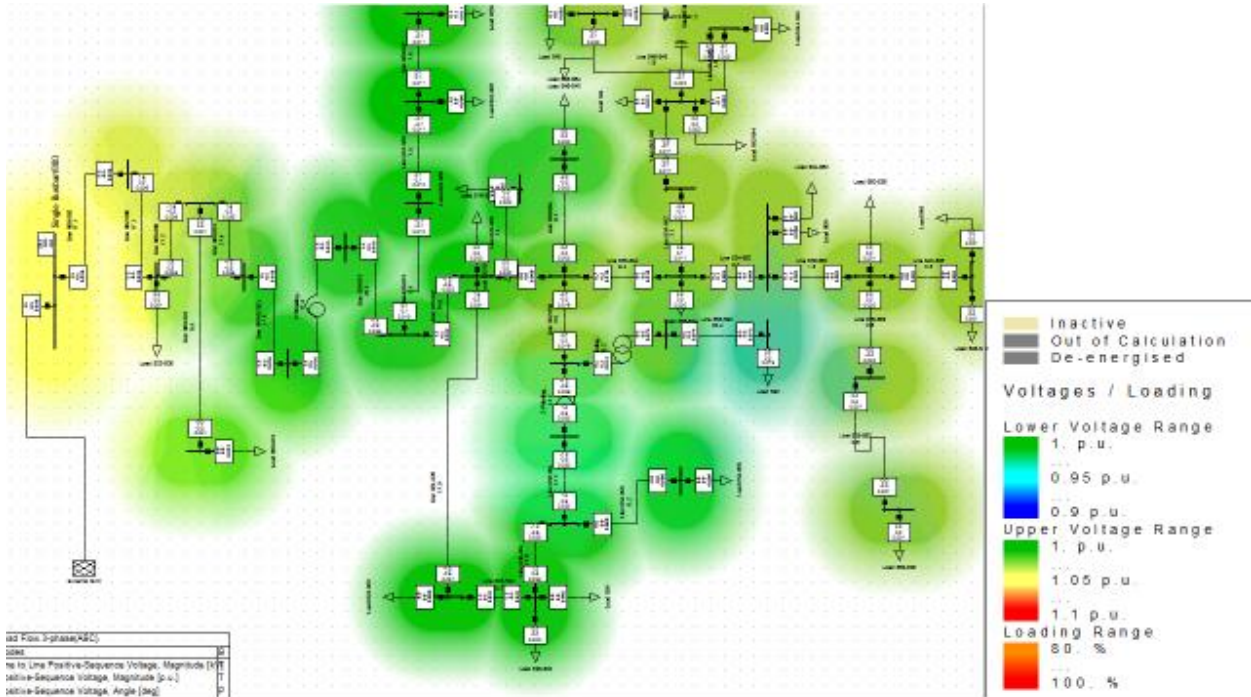


Figure 13: Heat map for the IEEE 34-node test system.

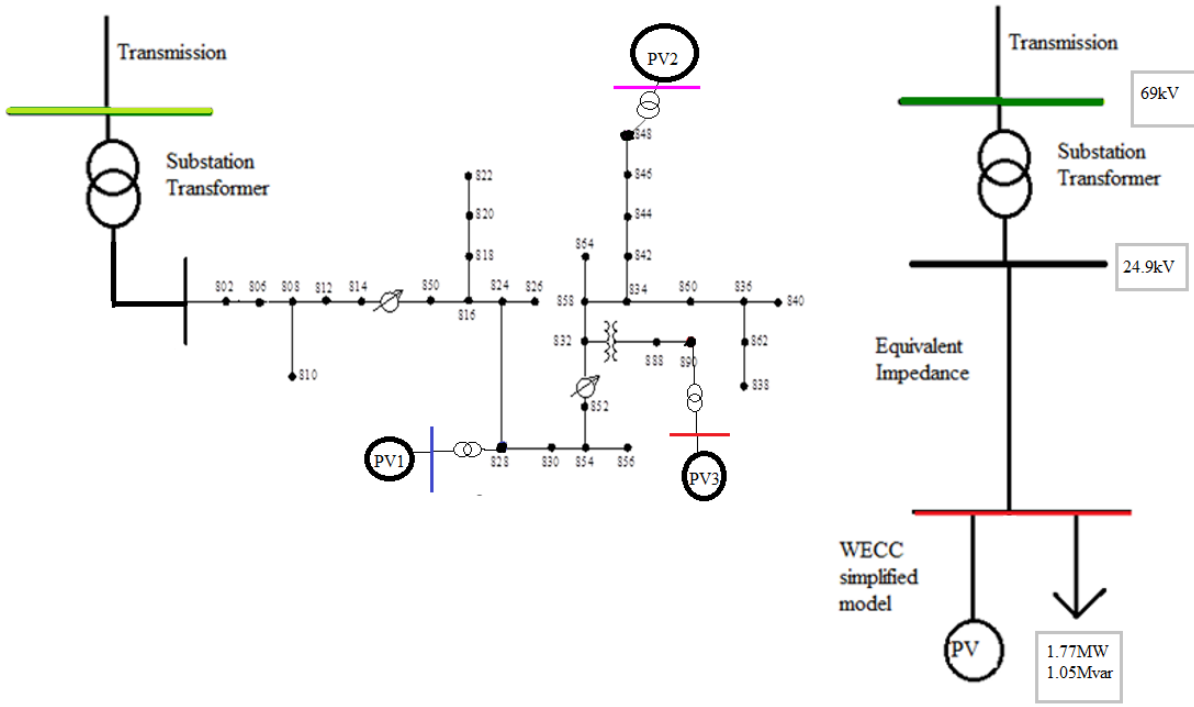


Figure 14: IEEE 34-node test system.

4.3 Results

The first modification to the test system was to add a substation to the test feeder. The high side of the transformer represents the transmission network. The temporary fault was applied to the transmission network and lasts for a duration of 0.2s. To test faults with different voltage drops the fault impedance was varied as explained in Appendix B. The second modification was to insert three instances of the extended PV model into the test feeder at various locations. Each PV model was set with the same rating of 0.56MVA. Figure 14 on the left side shows the modified test system. The base case setup has 100% PV penetration on instantaneous load, meaning that the power produced by the PV model equals the actual load consumed by the feeder. Each PV model covers one third of the total load of the test feeder.

Figure 15 shows the new voltage profile with 100% PV penetration. By comparing the 100% penetration results to the results in Figure 13 the high voltages are now at the far end of

the feeder. These are expected results because the power is flowing from the PV panels towards the grid. The feeder did not have to be upgrade with additional lines since the feeder is initially lightly loaded

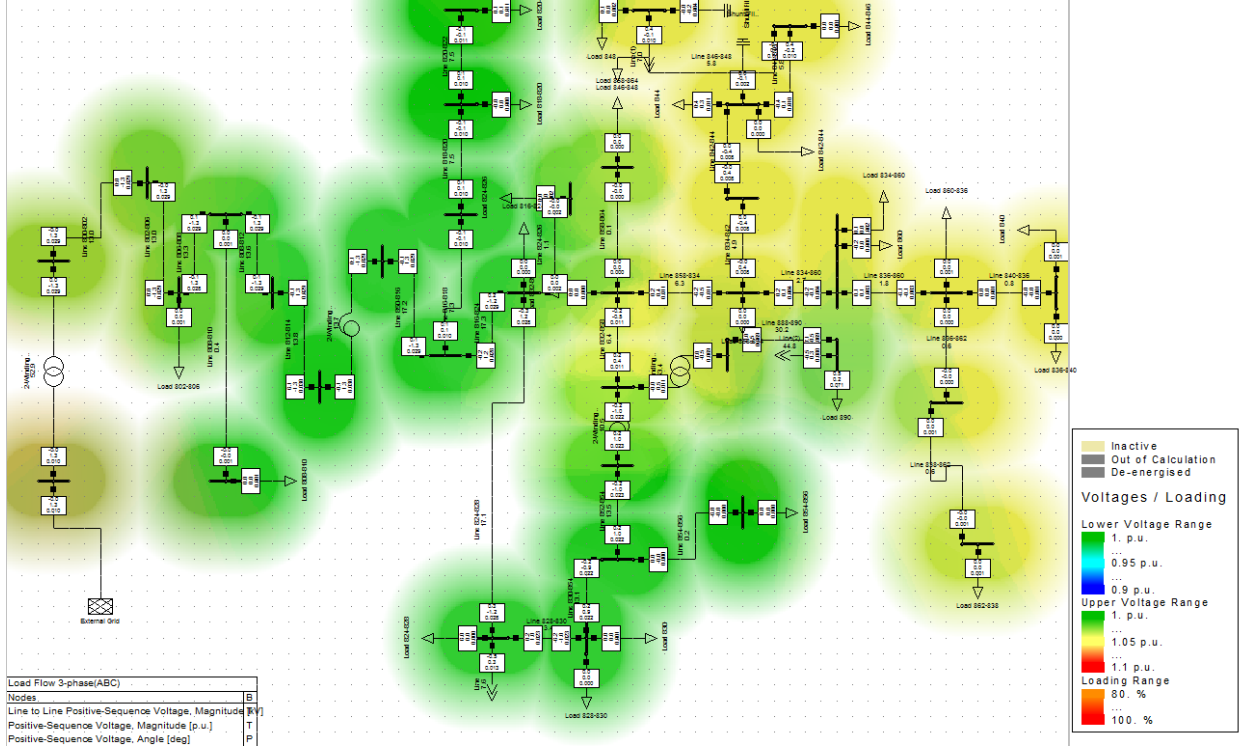


Figure 15: Voltage profile with 100% PV penetration.

For the simulations, PV1 was set to either LVRT or LVRT with dynamic voltage support while PV2 and PV3 were set to nLVRT. This equals a partial dropout rate of approx. 35%. Figure 14 shows the location of PV1, PV2, and PV3. Table 7 in Appendix A lists the values for the different ride through modes for the PV models. .

The WECC model, shown on the right side of Figure 14, is also set to LVRT and LVRT with dynamic voltage support. The model was set with Vrflag at 0.35 so that 35% of the PV returns post-fault to match PV1 in the extended model. Table 8 in Appendix A lists the values for the different ride through modes for the WECC simplified model. The load model is an aggregation of the load values from the IEEE 34-node test system. The power consumed by the

load is 1.4MW and 0.861MVar with 31% constant power, 33% constant current, and 36% constant impedance ZIP model.

4.3.1 LVRT

The first PV ride-through control mode explored was LVRT without dynamic voltage support. The light green line in Figure 16 represents the high voltage side of the transformer of the IEEE 34-node test feeder and the dark green line represents the high voltage side of the transformer of the WECC simplified model test setup. For both voltage dips, the PV panels are supplying 100% of the load pre-fault and no power was coming from the external grid. During the fault, there was no reactive power injection from the PV models. This was the expected results since the PV model has not dynamic voltage support. Post-fault the only PV model to recover is PV1, which was set to LVRT mode, and now the external grid is providing the extra power needed to balance the tripped PV2 and PV3 models. Similarly, in the WECC model, 33% of the aggregated PV recovers and the external grid was providing the extra power needed.

There are some differences between the IEEE test feeder and the WECC simplified model. The real power post-fault is different. This may be due the length of the line and the load value because it does not take into account losses. The reactive power pre- and post-fault also do not match, again because of the fact that the aggregated model does not account for losses. The next step will be to optimize the results so that the outputs are more accurate.

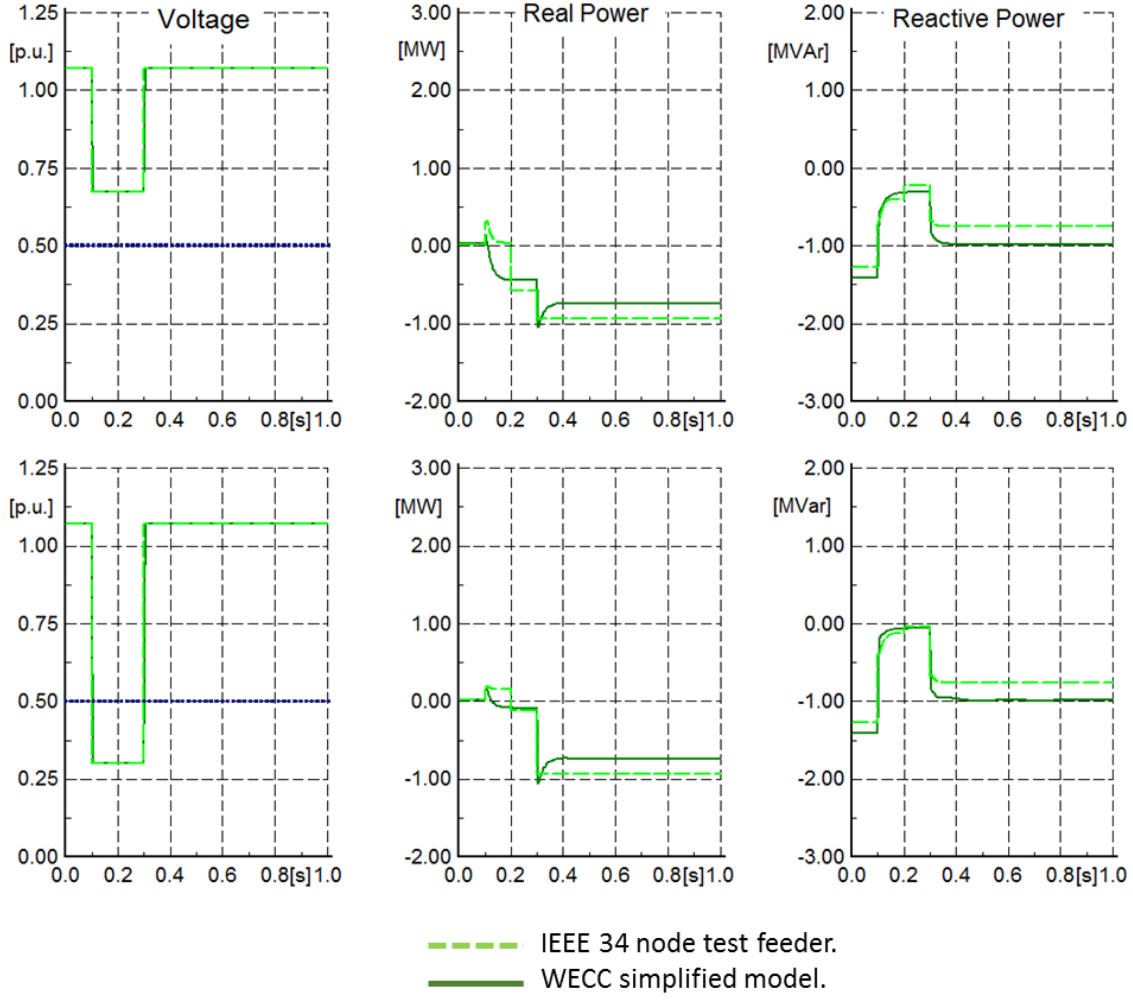


Figure 16: Results for LVRT North American network.

4.3.2 LVRT with Dynamic Voltage Support

To understand the effect of dynamic voltage support, PV1 was set to LVRT with Dynamic Voltage Support mode. The top three graphs in Figure 17 show the results for a voltage drop of 0.35pu (retained voltage of 0.65pu). The light green line represents the high voltage side of the transformer of the IEEE 34-node test feeder and the dark green line represents the high voltage side of the transformer of the WECC simplified model test setup. Pre-fault, the power coming from the external grid was zero due to 100% penetration of PV. During the fault, there was an increase of reactive power due to the dynamic voltage support. The impact of the increased reactive power was an increase in voltage during the fault. Post-fault the only PV to

return was the one set to LVRT mode with dynamic voltage support. The voltage drop was too large for the dynamic voltage support to prevent the other PV from dropping out post-fault. The WECC model has a higher percentage of the power returning post-fault due to the aggregated nature of the model and the parameters chosen for partial dropout (Vt0, Vt1).

The bottom three graphs in Figure 17 show the results for a voltage drop of 0.7pu (retained voltage of 0.3pu). Pre-fault the power coming from the external grid is zero due to 100% penetration of PV. During the fault, there was no increase in reactive power because the voltage falls below 0.5pu and PV1 switches to momentary cessation. Post-fault the only PV model to recover was PV1, which was set to LVRT mode with dynamic voltage support, and now the external grid is providing the extra power needed. With the WECC model, 33% of the aggregated PV recovers and the external grid was providing the extra power needed.

As in the LVRT case pre- and post-fault reactive powers do not match due to losses not associated with the aggregated model. However, the important thing to note is that the post-fault real power for the voltage drop of 0.35pu does not match because the WECC model reduces the generation in an amount proportional to the voltage deviation. This was because the IEEE test feeder only has three controllable PV models and not as fine of control of how much of the PV returns post-fault. Adding more distributed generation to the IEEE test feeder may improve the results.

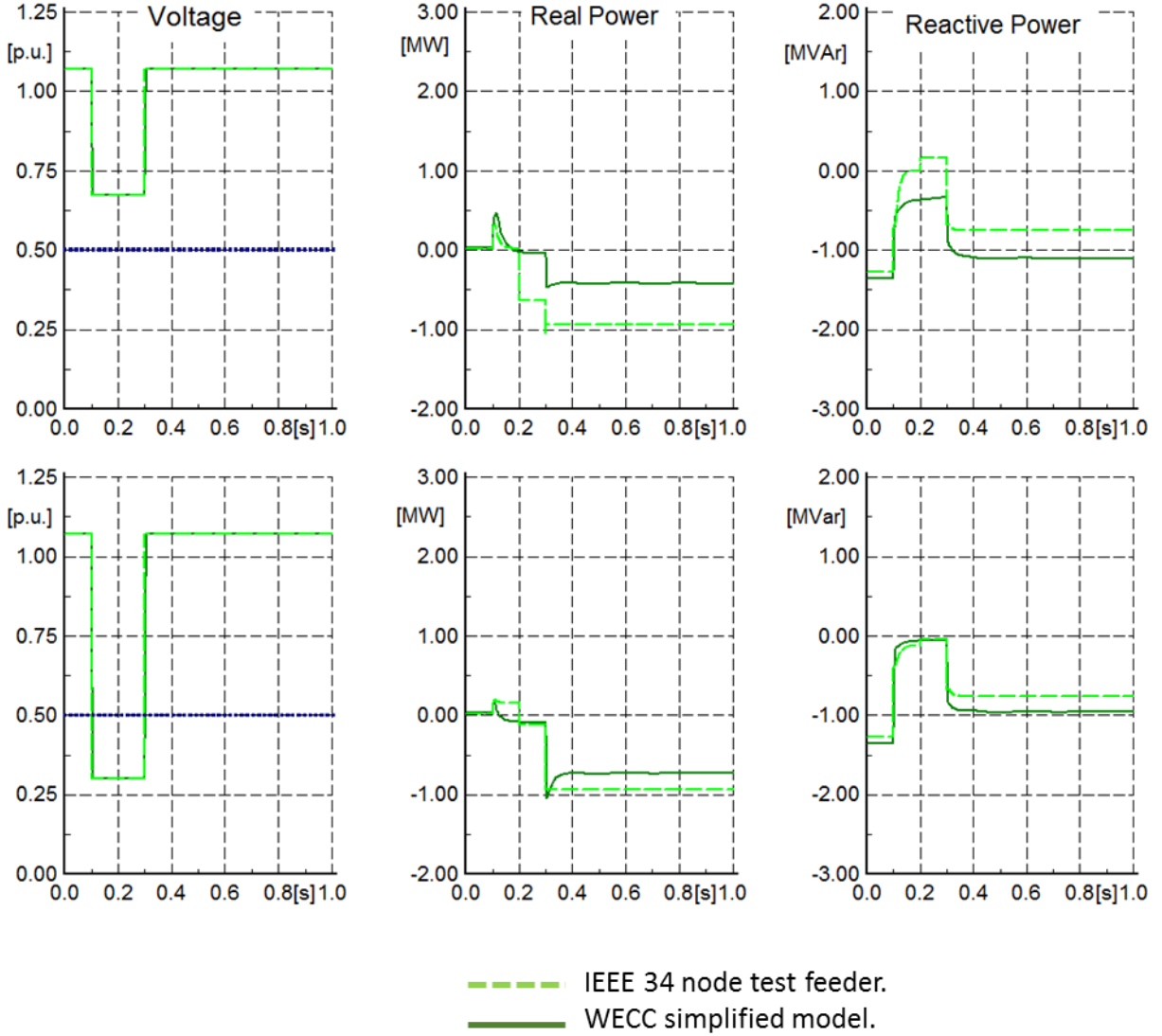


Figure 17: Results for LVRT with dynamic voltage support North American network.

4.4 Optimize WECC Simplified Model

An optimization algorithm was used to reduce the observed differences between the two simulations. The optimization algorithm is a mean variance mapping optimization (MVMO) developed in [21] that was applied to the WECC Simplified Model by [22]. The algorithm optimized the length of the equivalent distribution line, as well as the parameters Tg, Vrflag, Vt0, and Vt1 for the WECC simplified model. Table 3 lists six different cases to see the effect of location and ride through mode on the optimization results.

Table 3: List of optimized cases.

| Case | PV1 | PV2 | PV3 |
|-------------|---|---|---|
| 1 | LVRT | nLVRT | nLVRT |
| 2 | LVRT with Dynamic Voltage support | nLVRT | nLVRT |
| 3 | nLVRT | LVRT | nLVRT |
| 4 | nLVRT | LVRT with Dynamic Voltage support | nLVRT |
| 5 | nLVRT | nLVRT | LVRT |
| 6 | nLVRT | nLVRT | LVRT with Dynamic Voltage support |

Table 4 lists the base case values and Table 5 lists the optimized results. Looking at the results the biggest change from the base case values is T_g the inverter current lag time constant. For the cases with dynamic voltage support is about half the base case value while the LVRT cases the value is about twice the base case value. The length of the line needed to be increased significantly to make up for the losses. The total line length in the system is 93.91km, which is close to the optimized values. The even number cases which are with LVRT with dynamic voltage support, V_{t0} is optimized to the maximum allowed value. This is because the WECC simplified model is an aggregated model and it is trying to allow the maximum generation to remain connected post-fault. Otherwise, the values are adjusted slightly to improve the results.

Table 4: Base case values.

| Element | Parameters | Base LVRT | Base LVRT with dynamic voltage support |
|----------------|-----------------------|-----------|--|
| MV load | Active Power (MW) | 1.408 | 1.408 |
| | Reactive Power (MVar) | 0.861 | 0.861 |
| Line | Length (km) | 20 | 20 |
| WECC PVD model | Tg | 0.02 | 0.02 |
| | Vrflag | 0.33 | 0.33 |
| | Vt0 | 0.88 | 0.48 |
| | Vt1 | 0.9 | 0.9 |

Table 5: Optimized results for the WECC simplified model.

| Element | Parameters | Case 1 | Case 2 | Case 3 | Case 4 | Case 5 | Case 6 |
|----------------|-----------------------|--------|--------|---------|--------|---------|--------|
| MV load | Active Power (MW) | 1.2698 | 1.367 | 1.332 | 1.4 | 1.291 | 1.402 |
| | Reactive Power (MVar) | 0.843 | 0.817 | 0.828 | 0.82 | 0.845 | 0.8 |
| Line | Length (km) | 95.9 | 99.636 | 91.326 | 98.543 | 94.547 | 97.37 |
| WECC PVD model | Tg | 0.040 | 0.01 | 0.045 | 0.013 | 0.045 | 0.014 |
| | Vrflag | 0.304 | 0.316 | 0.336 | 0.321 | 0.3 | 0.314 |
| | Vt0 | 0.87 | 0.5 | 0.86469 | 0.5 | 0.86026 | 0.5 |
| | Vt1 | 0.8986 | 0.92 | 0.9034 | 0.92 | 0.88726 | 0.92 |

The optimized results for case one are shown in Figure 18. The light green line represents the values on the high side of the substation transformer for the IEEE test system with distributed generation. The dark green line represents the values on the high side of the substation transformer for the WECC Simplified Model. The results match more closely compared with the results in Figure 16. The real and reactive power pre- and post-fault match the IEEE test feeder results.

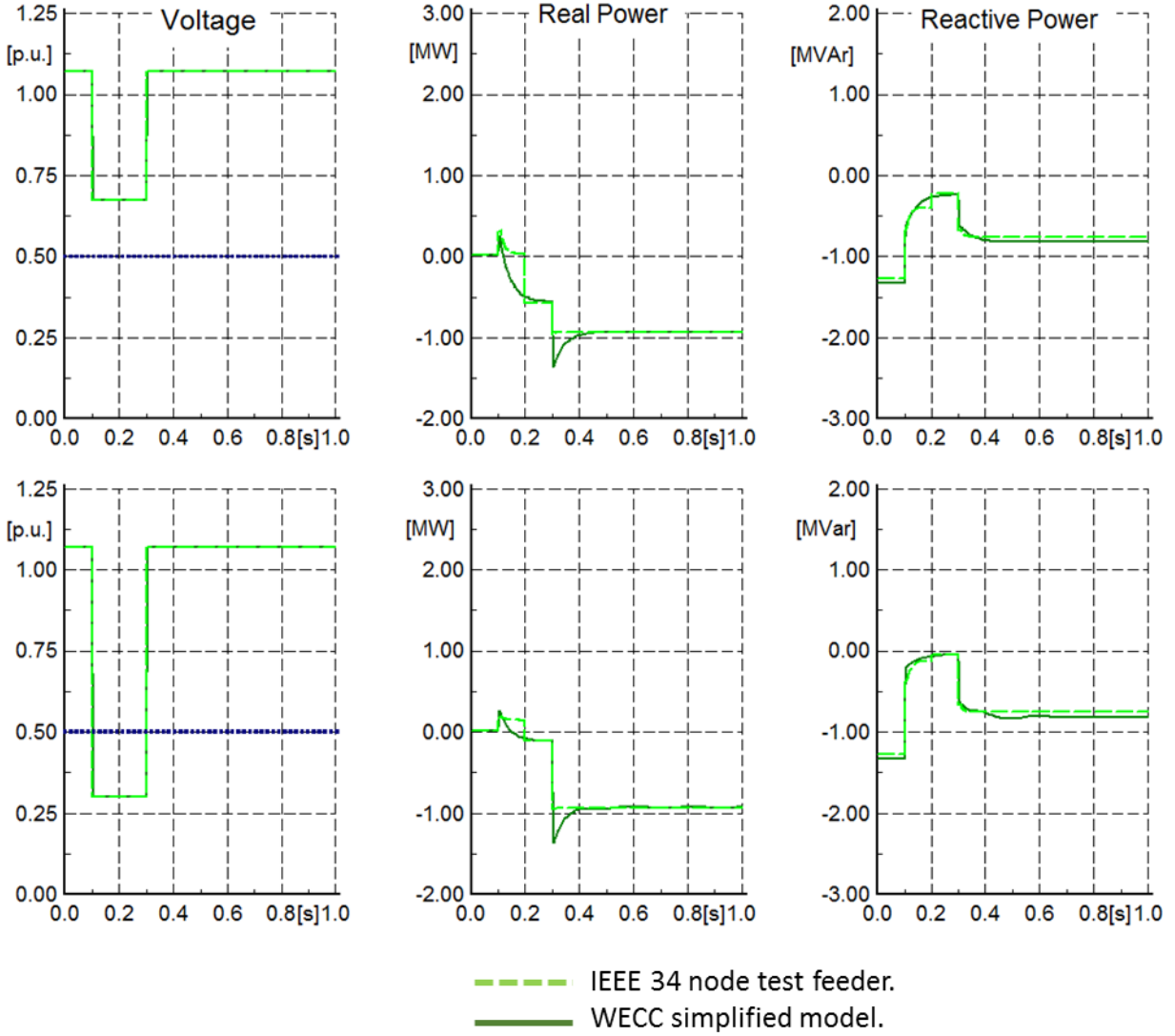


Figure 18: case 1 optimized results.

Figure 19 shows the results for case two. The main difference from case one is the PV model in ride through mode now provides dynamic voltage support during the fault. For the bottom three graphs when the voltage drops 0.7pu (retained voltage of 0.3pu), the real and reactive power values are the same. Though for the top three graphs when the voltage drops to 0.35pu (retained voltage of 0.65pu), the real and reactive power does not match post-fault. This is because the WECC simplified model reduces the generation in an amount proportional to the voltage deviation. While the IEEE test feeder with distributed generation does not have as fine a

control. The reactive power of the WECC simplified model does not increase because it is not correctly modeling the dynamic voltage support compared to the extended PV model.

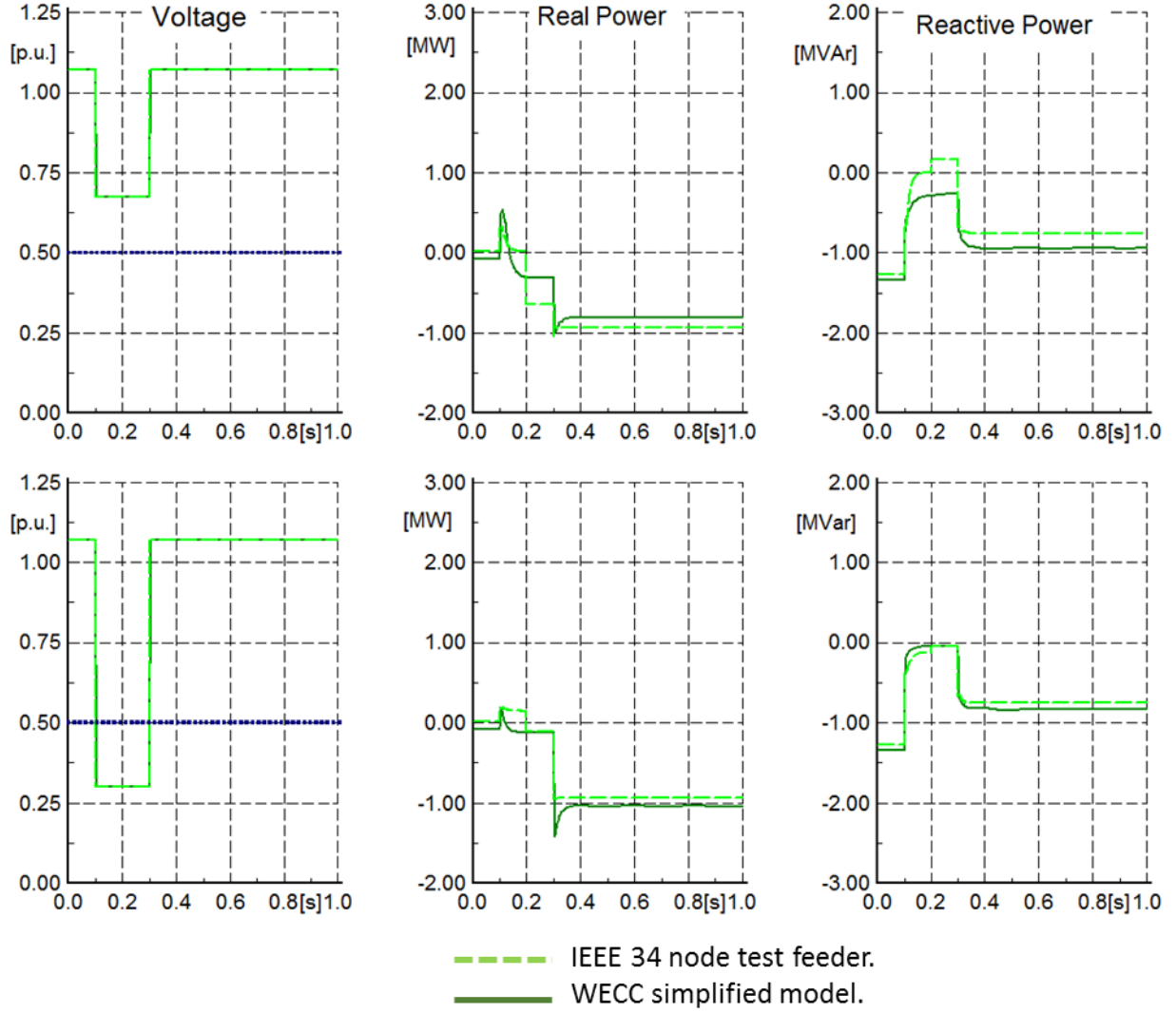


Figure 19: case 2 optimized results.

4.5 Benefit of IEEE 1547 Standard

To evaluate the effectiveness of the proposed revisions to the IEEE 1547 standard, a voltage drop of 0.11pu (retained voltage to 0.89pu) was applied to see if the extended PV model with dynamic voltage support would allow more PV to remain connected post-fault. The top three graphs of Figure 20 (a) are PV1 in LVRT with dynamic voltage support, the middle three graphs (b) are PV2 in LVRT with dynamic voltage support, and the bottom three graphs (c) are

PV3 in LVRT with dynamic voltage support. The salient result is that for (a) and (c) the dynamic voltage support allows more of the PV to remain connected post-fault while for (b) the location of the PV with dynamic voltage support does not support the system with a higher amount of PV remaining connected post-fault.

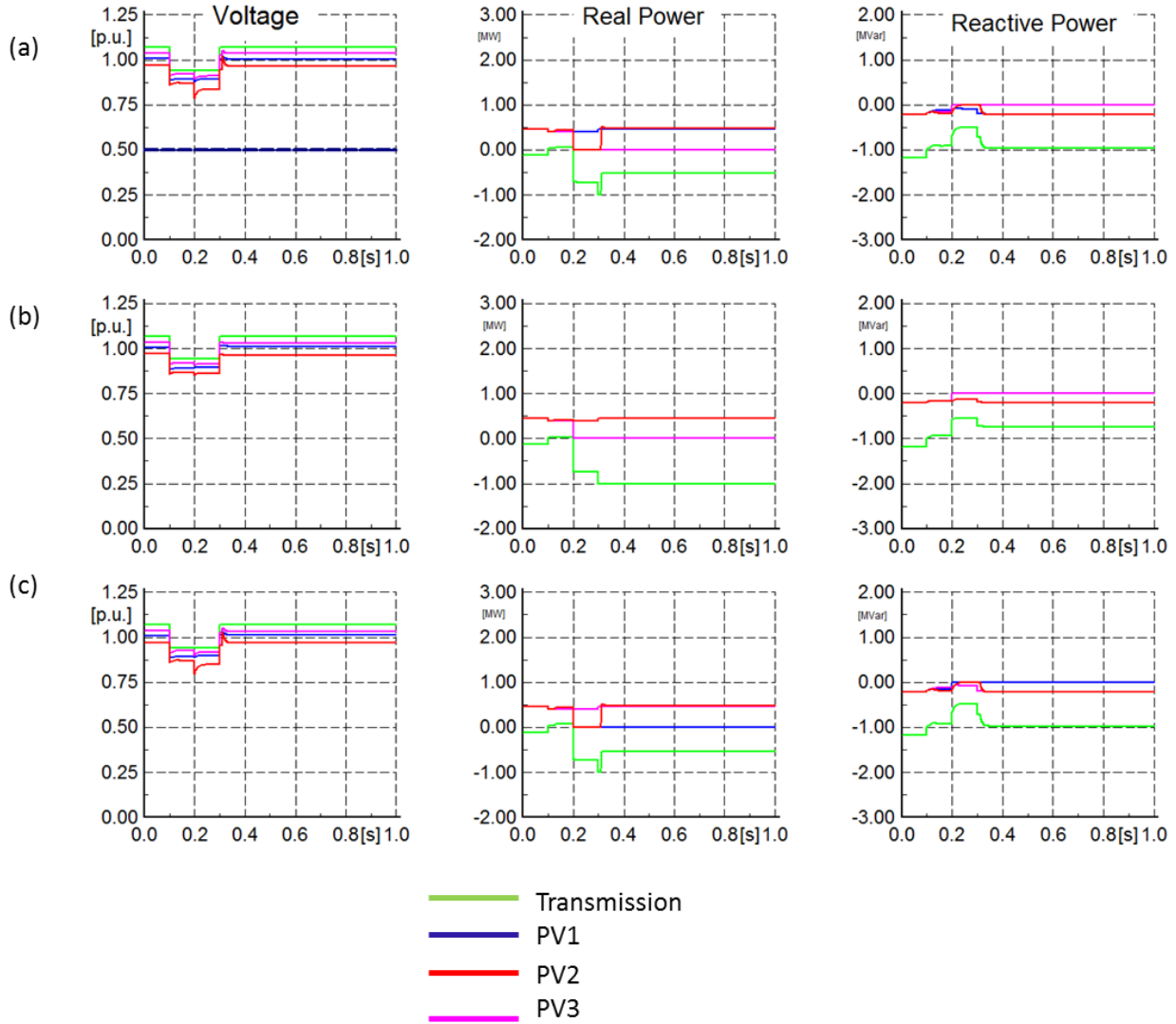


Figure 20: Results for the benefit of the IEEE 1547 standard.

After 0.1s, the PV models in nLVRT mode disconnect leading to the voltage drop seen in Figure 20. According to [23] the reason the voltage drops after disconnection is the increased

power flowing across the transformer. Post-fault the only PV model to recover is PV1, which is set to LVRT mode, and now the external grid is providing the extra power needed.

The same comparison for the WECC simplified model was made this time with a voltage drop of 0.25pu (retained voltage of 0.75pu) to see if the WECC model with dynamic voltage support had the same effect on the PV recovery as the extended PV model. Figure 20 (a) is with dynamic voltage support and (b) is without. The pre-fault values are the same for both (a) and (b). During the fault, in (a) the dynamic voltage support increases the reactive power. Figure 21 (a) post-fault 80% of the PV are still connected post-fault compared with (b) 33% is connected post-fault. These results show that with the proposed revisions to IEEE 1547 standard more PV returns post-fault. This decrease in the amount of PV dropping out will increase the stability of the system.

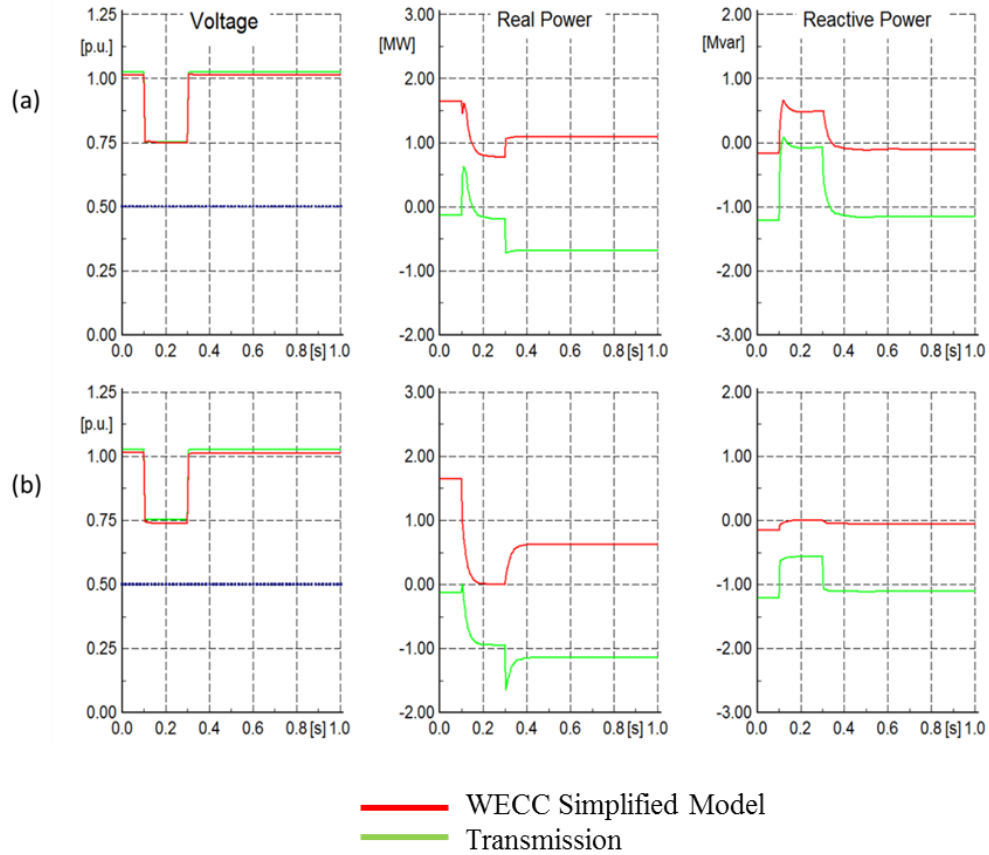


Figure 21: WECC model results for the benefit of IEEE 1547 standard.

5. Conclusion and Recommendations

The existing wind and PV models were extended to allow them to model the proposed IEEE P1547 ride-through requirements based on the concept of voltage-dependent operating regions. This involved adding an additional deadband so the models would go into momentary cessation and stop providing dynamic voltage support but still remain connected post-fault. The modeling results for two meaningful voltage sags suggest a stable operation of distributed PV systems with next generation interconnection requirements including dynamic voltage support. The WECC simplified model was implemented in PowerFactory. The results were compared to the extended PV model to verify the model was implemented correctly; certain model limitations were found, especially for the behavior in the fault period.

A typical North American distribution network was modeled with distributed PV panels integrated at various locations. Partial dropout of PV panels due to transmission voltage sags were analyzed. The dynamic response of this North American distribution network was compared with the response of the WECC distributed PV model to identify the limitations and optimal parameters of the WECC model. The WECC model allows for modeling of DERs in large-scale bulk system stability studies at a lower computational cost. The results show that the WECC model does not model what was occurring during the fault. The pre- and post-fault values match for the case of the LVRT. However, for the case of dynamic voltage support the post-fault values do not match since the WECC model reduces the power infeed during the fault in the amount proportional to the voltage deviation. The North American Distribution network is superior but the PV models do not have as fine a control because there are only three distinct models in the network.

The results for the WECC model were optimized so that the results matched the North American distribution network in the post-fault period. The optimization results showed that the

WECC model can be adjusted to match a typical North American distribution network. As demonstrated before, the North American Distribution network PV models do not have as fine of control for the dynamic voltage control and the results do not match perfectly.

The proposed requirements on dynamic voltage support from the IEEE P1547 draft standard were evaluated to see if they would help improve the stability of the system. It was found that the dynamic voltage support might increase the amount of power that returned post-fault. While stringent voltage ride-through requirements are of overall importance, dynamic voltage support can additionally help raise the voltage of nLVRT PV panels above their under-voltage trip threshold in certain areas of a transmission voltage sag.

Future research should increase the number of PV panels connected to the IEEE 34-node test feeder to assess the accuracy of the current setup in a more realistic setup. It would also be interesting to look at the effects of using a larger IEEE test feeder and see the effects on a large-scale bulk power system. These adjustments could also give a better understanding of the effects of the proposed IEEE P1547 requirements. Future work may include a closer look at aggregation techniques for DER. This could include other aggregated models and see how they compare to the WECC model. It would be good to find a model that better models the dynamic behavior during the fault. Finally, it would be interesting to do the same study for an aggregated wind model.

Reference

- [1] Efta.int,.2015. 'European Economic Area European Free Trade Association'.
<http://www.efta.int/eea>.
- [2] J. G. Slootweg and W. L. Kling, "Impacts of distributed generation on power system transient stability" Power Engineering Society Summer Meeting, 2002 IEEE", Power Engineering Society Summer Meeting, 2002 IEEE, vol. 2, pp. 862-867 vol.2, 2002.
- [3] Electric Power Research Institute (EPRI),. 2015. *Recommended Settings for Voltage and Frequency ride-Through of Distributed Energy Resources*.
- [4] *Standard for Interconnecting Distributed Resources with Electric Power Systems* (IEEE Std. 1547-2003). IEEE Standards Coordinating Committee 21, 2003.
- [5] G. Papaefthymiou, R. Kuwahata, M. Doering, and K. Burges et al., "Assessment of the Frequency Settings from Distributed Generation in Germany for the Prevention of Frequency Stability Problems in Abnormal System Conditions," presented at the 12th International Workshop on Large-Scale Integration of Wind Power into Power Systems as well as on Transmission Networks for Offshore Wind Power Farms, London, U.K. (October 2013).
- [6] B. Weise, "Impact of K-factor and active current reduction during fault-ride-through of generating units connected via voltage-sourced converters on power system stability," IET RENEWABLE POWER GENERATION. Vol. 9, No. 1, p. 25-36 92015).
- [7] *Software Based Challenges of Developing the Future Distribution Grid*. LBNL. Lawrence Berkeley National Laboratory: June 2014. Report LBNL 6708E,
<http://eetd.lbl.gov/publications/software-based-challenges-of-developi>.
- [8] *Draft Standard for Interconnecting Distributed Resources with Electric Power Systems* (IEEE P1547). Draft 3 (January 2016). IEEE Standards Coordinating Committee 21, 2016,
http://grouper.ieee.org/groups/scc21/1547_revision/1547revision_index.html.
- [9] CPUC, "Interconnection (Rule 21)". Accessed January 21, 2015,
<http://www.cpuc.ca.gov/PUC/energy/rule21.htm>.
- [10] *Transient Over-Voltage and Frequency & Voltage Ride -Through Requirements for Inverter-Based Distributed Generation Projects*. HECO. Hawaiian Electric Companies: February 2015,
http://www.hawaiianelectric.com/vcmcontent/StaticFiles/pdf/TrOVandFVRT_Public_Feb2015.pdf.
- [11] *Wind turbines-Part 27-1: Electrical simulation models-Wind turbines* (IEC 61400-27-1). IEC ICS 27.180: 2015, 2015.
- [12] DigSILENT GmbH, "Fully Rated WTG Template: Manual", Gomaringen, Germany, May 2011.
- [13] J.C. Boemer, B.G. Rawn, M. Gibescu, and M.A. van der Meijden et al., "Response of Wind Power Park Modules in Distribution Systems to Transmission Network Faults during Reverse Power Flows," *IET Renewable Power Generation*, 9 (no.8) (November 2015): 1033–42.
- [14] K. Skaloumpakas, "Response of Low Voltage Networks with High Photovoltaic Systems Penetration to Transmission Network Faults," Master thesis, Electrical Sustainable Energy,

Delft University of Technology, January 29, 2014,
<http://repository.tudelft.nl/view/ir/uuid%3Abf0a92ff-2a9f-4e26-8044-e509550a5998/>.

- [15] S.I. Nanou, and S.A. Papathanassiou, "Modeling of a PV system with grid code compatibility," *Electric Power Systems Research* 116 (2014): 301-10.
- [16] Dugan, Roger. 'Distribution Test Feeders - Distribution Test Feeder Working Group - IEEE PES Distribution System Analysis Subcommittee'. Ewh.ieee.org.
- [17] WECC PV Power Plant Dynamic Modeling Guide,. WECC Renewable Energy Modeling Task Force. Western Electricity Coordinating Council: April 2014.
- [18] E. van Ruitenbeek, "Impact of Large Amounts of Photovoltaic Installations in Low-Voltage Networks on Power System Stability During Transmission System Faults,". Master thesis, Electrical Sustainable Energy, Delft University of Technology, June 17, 2014, <http://resolver.tudelft.nl/uuid:cffa6cde-faeb-47b9-9023-210778b0a0d2>.
- [19] CIGRE Task Force C6.04.02 *Benchmark Systems for Network Integration of Renewable and Distributed Energy Resources*: Technical Brochure. Paris (21 rue d'Artois, 75008): COGRE, 2014.
- [20] W.H. Kerstin, "Distribution system Modeling and Analysis", FL: CRC Press LLC, 2012.
- [21] J.L. Rueda, J. Cepeda, I. Erlich, and D. Echeverría et al., "Heuristic optimization based approach for identification of power system dynamic equivalents," *International Journal of Electrical Power & Energy Systems* 64 (2015): 185–93. doi:10.1016/j.ijepes.2014.07.012.
- [22] D. Gusain, J.L. Rueda, J.C. Boemer, and P. Palensky, "Identification of Dynamic Equivalents of Active Distribution Networks through MVMO," *Workshop on Control of Transmission and Distribution Smart Grids (CTDSG '16), 11-13 October 2016, Prague, Czech Republic*, Paper submitted for presentation. Accessed May 2, 2016.
- [23] K. Skaloumpakas, J.C. Boemer, E. van Ruitenbeek, and M. Gibescu et al., "Response of Low Voltage Networks with High Penetration of Photovoltaic Systems to Transmission Network Faults," presented at the 3rd Renewable Power Generation Conference (RPG 2014), Naples, Italy (24-25 September, 2014), 8.27., 2014.
- [24] *P1547 Project Authorization Request: Revision to IEEE Standard 1547-2003*. IEEE Standards Coordinating Committee 21. IEEE: March 27, 2014, http://grouper.ieee.org/groups/scc21/1547_revision/1547revision_index.html.
- [25] *Performance of Distributed Energy Resources During and After System Disturbance: Voltage and Frequency ride-Through requirements*. North American Electric Reliability Corporation: December 2013.
- [26] *The Technical Basis for the New WECC Voltage Ride-through (VRT) Standard: A White Paper Developed by the Wind Generation Task Force (WGTF)*, Western Electricity Coordinating Council: June 13, 2007.
- [27] *Interconnection of Wind Energy* (Order No. 661-A). Federal Energy Regulatory Commission, 2005.
- [28] S. Sugita, Y. Kataoka, S. Naoi, and Y. Noro et al., "Study of modeling method distributed generators considering partial dropout for trunk transmission system," presented at the

2010 International Power Electronics Conference-ECCE Asia, Sapporo, Japan (June 21-24, 2010), 975-80. [Piscataway, N.J.]: IEEE, 2010.

Appendix A

Tables

Table 6: Wind model parameters.

| | Description | nLVRT | LVRT | LVRT with Dynamic Voltage Support |
|--------------------------|---|-------|-------|-----------------------------------|
| Kp | Active power control gain | 0.5 | 0.5 | 0.5 |
| Tp | Active power control time constant | 0.05 | 0.05 | 0.05 |
| Kq | Reactive power control gain | 0.5 | 0.5 | 0.5 |
| Tq | Reactive power control time constant | 0.5 | 0.5 | 0.5 |
| Xm | Magnetizing reactance @pbase | 0.0 | 0.0 | 0.0 |
| FRT_db_FAULT | Voltage deadband for fault detection (hysteresis low) | 0.13 | 0.13 | 0.13 |
| FRT_db_CLEAR | Voltage deadband for fault clearance (hysteresis high) | 0.11 | 0.11 | 0.11 |
| FRT_db_LOW | Voltage deadband for low voltage clearance | 0.5 | 0.5 | 0.5 |
| i_FRT_CI_DB | 0=TC curve; 1=SDL curve | 0.0 | 0.0 | 1.0 |
| FRT_Tvid | Voltage-dependent id-reduction control time Constant | 0.005 | 0.005 | 0.005 |
| FRT_Tdetect | Time to detect a fault: Voltage Support Delay | 0.01 | 0.01 | 0.01 |
| i_FRT_CI_CONT | Current injection continuation Period after fault for FRT_CI_Tcont: 0=no; 1=yes | 1.0 | 1.0 | 1.0 |
| FRT_CI_Tcount | Voltage Support Continuation Period after fault for i_FRT_CI_CONT=1 | 10.0 | 0.01 | 0.5 |
| FRT_CI_k | Short-circuit Current Gain | 0.0 | 0.0 | 6.0 |
| i_max | Combined current limit | 1.2 | 1.2 | 1.2 |
| i_FRT_CI_MOD | Current injection during fault: 0=total (TC mode); 1=additional to pre-fault value (SDL mode) | 0.0 | 0.0 | 1.0 |
| i_FRT_CI_PRIO | Current priority given to 0=id; 1=iq (TC & SDL mode); other =equal (RACI mode) | 0.0 | 1.0 | 1.0 |
| i_FRT_CI_PRIO_MOD | Current priority mode: 1=arithmetic (abs); 2=geometric (sqrt); other=set other value to zero | 0.0 | 3.0 | 1.0 |

| | | | | |
|----------------------|--|-------|-------|-------|
| i_FRT_CI_STAB | Stability improvement during fault by voltage dependent id reduction: 0=no; 1=yes | 0.0 | 0.0 | 0.0 |
| i_FRT_CI_ANG | Current angle (a)RACI, best set equal to phiz=arg(Z_grid) | 90.0 | 90.0 | 90.0 |
| i_FRT_dAPR | Delayed active power recovery after fault for FRT_dAPR_ramp: 0=no; 1=yes | 0.0 | 1.0 | 1.0 |
| FRT_dRPR_ramp | Active Power Ramp after fault is cleared | 200.0 | 200.0 | 200.0 |
| u_max | max. allowed internal voltage | 1.1 | 1.1 | 1.1 |
| X | Coupling Reactance | 10 | 10 | 10 |
| id_max | id current limit | 1.15 | 1.15 | 1.15 |
| iq_max | iq current limit | 1.15 | 1.15 | 1.15 |

Table 7: PV model parameters.

| | Description | nLVRT | LVRT | LVRT with dynamic voltage support |
|-------------------|--|-----------|-----------|-----------------------------------|
| Tfac | AC Voltage Filter Time Constant | 0.002 | 0.002 | 0.002 |
| Tqfac1 | (Directly controlled) q-axis current filter time constant | 0.001 | 0.001 | 0.001 |
| Ibase | Base current is which all PI controller parameters are tuned | 0.0507 | 0.0507 | 0.0507 |
| i_FRT_APR | Active power recovery delay after fault (1=ON, 0=OFF) | 0.0 | 0.0 | 0.0 |
| i_FRT_Mode | 0=NlVRT; 1=ZPM; 2=aRCI; 3=a(R+A) | 0.0 | 1.0 | 2.0 |
| CITqfac | Reactive Power Filter Time Constant | 0.001 | 0.001 | 0.001 |
| Kdc | DC voltage Controller | -12976.0 | -12976.0 | -12976.0 |
| GainKqac | Reactive power Controller | -0.226755 | -0.226755 | -0.226755 |
| GainTqac | Reactive power Controller Time Constant | 0.002205 | 0.002205 | 0.002205 |
| Kac | AC voltage controller | -0.5 | -0.5 | -0.5 |
| GainTac | AC voltage controller time constant | 0.001 | 0.001 | 0.001 |
| Tfdc | DC voltage controller time constant | 0.0 | 0.0 | 0.0 |
| Tdc | DC voltage filter time constant | 300.0 | 300.0 | 300.0 |
| Tlg | DC voltage controller time lag constant | 0.0011 | 0.0011 | 0.0011 |

| | | | | |
|---------------------------|---|------------|------------|------------|
| Tld | DC voltage controller time lead constant | 0.02323 | 0.02323 | 0.02323 |
| G | Gain of lead lag block in DC voltage | 1.0 | 1.0 | 1.0 |
| PI controli_Q_Mode | 0=reactive power; 1=Vac; 2=Direct_iqref | 0.0 | 0.0 | 0.0 |
| deadband | Deadband for fast voltage control | 0.1 | 0.1 | 0.1 |
| deadband_low | Momentary cessation deadband limit | 0.5 | 0.5 | 0.5 |
| Imax | Maximum total current during fast voltage control | 1.1 | 1.1 | 1.1 |
| K_id | Gain for aACI | 0 | 10 | 10 |
| Karci | Gain for aRCI | 0 | 10 | 10 |
| Angle | Angle for aA/RCI | 90.0 | 90.0 | 90.0 |
| Tdrop | Only in nLVRT mode: resynchronization time constant | 60.0 | 60.0 | 60.0 |
| Trelay | Delay time for returning to normal operating mode after faults | 0.1 | 0.1 | 0.1 |
| K | 1 st order filter gain for aACI only | 1.0 | 1.0 | 1.0 |
| T | 1 st order filter time constant for aACI only | 0.01301236 | 0.01301236 | 0.01301236 |
| Tsr | Delay time for returning to normal operating mode after faults | 0.0 | 0.0 | 0.0 |
| K1 | 1 st order filter gain for aRCI only | 1.0 | 1.0 | 1.0 |
| T1 | 1 st order filter time constant for a RCI only | 0.01301236 | 0.01301236 | 0.01301236 |
| Vb | d-axis current control DC base voltage | 0.4718 | 0.4718 | 0.4718 |
| iq_min | Minimum Current | -0.02218 | -0.02218 | -0.02218 |
| Outputi_min | Minimum Current Output | 0.0 | 0.0 | 0.0 |
| Min_iq | Lower limit for q-axis current for Flag=2=Direct_iqret control strategy | -0.507 | -0.507 | -0.507 |
| iq_max | Maximum Current | 0.02218 | 0.02218 | 0.02218 |
| Outputi_max | Maximum Current Output | 0.0507 | 0.0507 | 0.0507 |
| Max_iq | Upper limit for q-axis current for Flag=2=Direct_iqret control strategy | 0.0507 | 0.0507 | 0.0507 |

Table 8: WECC simplified model parameters.

| | Description | nLVRT | LVRT | LVRT with dynamic voltage support |
|-----------|------------------------------------|-------|------|-----------------------------------|
| Tg | Inverter current lag time constant | 0.02 | 0.02 | 0.02 |

| | | | | |
|------------------------|--|--------|--------|--------|
| I_{max} | Apparent current limit | 1.2 | 1.2 | 1.2 |
| Pqflag | Priority to reactive current (0) or active current (1) | 1.0 | 1.0 | 0.0 |
| Vrflag | Voltage tripping is latching (0) or partially self-resetting (>0 and ≤ 1) | 0.0 | 0.35 | 0.35 |
| Vt0 | Voltage tripping response curve point 0 | 0.88 | 0.88 | 0.48 |
| Vt1 | Voltage tripping response curve point 1 | 0.9 | 0.9 | 0.9 |
| Vt2 | Voltage tripping response curve point 2 | 1.1 | 1.1 | 1.1 |
| Vt3 | Voltage tripping response curve point 3 | 1.2 | 1.2 | 1.2 |
| Frflag | Frequency tripping is latching (0) or partially self-resetting (>0 and ≤ 1) | 0.0 | 0.35 | 0.35 |
| Ft0 | Frequency tripping response curve point 0 | 59.5 | 59.5 | 59.5 |
| Ft1 | Frequency tripping response curve point 1 | 59.7 | 59.7 | 59.7 |
| Ft2 | Frequency tripping response curve point 2 | 60.3 | 60.3 | 60.3 |
| Ft3 | Frequency tripping response curve point 3 | 60.5 | 60.5 | 60.5 |
| V0 | Lower limit of deadband for voltage droop response | 0.9 | 0.98 | 0.98 |
| V1 | Upper limit of deadband for voltage droop response | 1.1 | 1.02 | 1.02 |
| Dqdv | Voltage droop response characteristic | 0.0 | 12.5 | 12.5 |
| Ddn | Down regulation droop gain | 0.0 | 0.05 | 0.05 |
| Fdbd | Overfrequency deadband for governor response | 0.1 | 0.1 | 0.1 |
| Xc | Line drop compensation reactance | 0.0 | 0.0 | 0.0 |
| Qmn | Minimum reactive power command | -0.328 | -0.328 | -0.328 |
| Qmx | Maximum reactive power command | 0.328 | 0.328 | 0.328 |

Table 9: Error between IEEE voltages and voltages found in PowerFactory.

| | Phase A % | Phase B % | Phase C % |
|-----|-----------|-----------|-----------|
| 800 | 0.0004 | 0.0006 | 0.0010 |
| 802 | 0.0880 | 0.0374 | 0.0314 |
| 806 | 0.1593 | 0.0559 | 0.0448 |
| 808 | 1.3843 | 0.3609 | 0.3378 |
| 810 | 0.0000 | 0.3776 | 0.0000 |
| 812 | 2.8921 | 0.6443 | 0.7073 |
| 814 | 4.1600 | 0.8609 | 1.0131 |
| 816 | 1.4600 | 0.5231 | 0.4014 |
| 818 | 1.3877 | 0.0000 | 0.0000 |
| 820 | 0.5152 | 0.0000 | 0.0000 |
| 822 | 0.6935 | 0.0000 | 0.0000 |
| 824 | 1.1948 | 0.3302 | 0.2527 |
| 826 | 0.0000 | 0.3146 | 0.0000 |
| 828 | 1.1667 | 0.3186 | 0.2402 |
| 830 | 0.6215 | 0.0498 | 0.0725 |
| 832 | 1.3294 | 0.1637 | 0.4954 |
| 834 | 1.2147 | 0.0331 | 0.3759 |
| 836 | 1.1928 | 0.0094 | 0.3563 |
| 838 | 0.0000 | 0.0080 | 0.0000 |
| 840 | 1.1948 | 0.0068 | 0.3587 |
| 842 | 1.2777 | 0.0912 | 0.4348 |
| 844 | 1.2890 | 0.0949 | 0.4440 |
| 846 | 1.3083 | 0.0992 | 0.4691 |
| 848 | 1.3179 | 0.0989 | 0.4786 |
| 850 | 1.4719 | 0.5230 | 0.4099 |
| 852 | 0.3660 | 0.4347 | 0.6385 |
| 854 | 0.6116 | 0.0450 | 0.0785 |
| 856 | 0.0000 | 0.0332 | 0.0000 |
| 858 | 1.2770 | 0.1032 | 0.4365 |
| 860 | 1.1976 | 0.0106 | 0.3650 |
| 862 | 1.1934 | 0.0019 | 0.3544 |
| 864 | 1.2771 | 0.0000 | 0.0000 |
| 888 | 0.3180 | 1.5127 | 1.1618 |
| 890 | 1.2069 | 2.5268 | 2.0948 |

Appendix B

Procedures

Calculating the retained voltage

1. Change the value of the short circuit power in the RMS simulation of the external grid to 2000MVA.
2. Calculate Z_{base} using $Z_{base} = \frac{S^2}{V}$ where S is the 2000MVA and V is the voltage at the bus which the fault is applied.
3. Calculate Z_{sc} using $Z_{sc} = \frac{V_{ret}}{1-V_{ret}} * Z_{base}$
4. Use Z_{sc} value for the fault reactance for a three phase to ground fault.

Step up the number of PV panels

1. 2-winding transformer: update the number of parallel transformers.
2. PWM convertor: update the number of parallel convertors.
3. DC-current source: multiply the nominal current by the number of parallel machines.
4. Shunt/filter: multiply the number of steps by the number of parallel machines.
5. PQ measurement: multiply the power rating by the number of parallel machines.
6. Mark ‘out of service’ the following models:
 - a. Active Power Frequency Reduction
 - b. Maximum Power Point Tracker
 - c. PV Module
 - d. PV Radiation
 - e. PV temperature

PV model in constant voltage mode

1. Power Factor Control Options module
 - a. PF_select: 2
2. PWM Converter load flow:
 - a. Control mode: Vdc-Vac
 - b. AC Voltage Setpoint: 0.95